GOLVEN peptides regulate lateral root spacing as part of a negative feedback loop on the establishment of auxin maxima

Joris Jourquin[1,2], Ana Ibis Fernandez[1,2], Qing Wang[1,2], Ke Xu[1,2], Jian Chen[1,2,4], Jan Šimura[3], Karin Ljung[3], Steffen Vanneste[4] & Tom Beeckman[1,2*]

[1] Department of Plant Biotechnology and Bioinformatics, Faculty of Sciences, Ghent University, Ghent 9052, Belgium

[2] Center for Plant Systems Biology, VIB-UGent, Ghent 9052, Belgium

[3] Department of Forest Genetics and Plant Physiology, Umeå Plant Science Centre, Swedish University of Agricultural Sciences, 90183 Umeå, Sweden

[4] Department of Plants and Crops, Faculty of Bioscience Engineering, Ghent University, Ghent 9000, Belgium

*Correspondence: tom.beeckman@psb.vib-ugent.be / +32(0)93313830

Highlight

GOLVEN peptides regulate the spacing of lateral roots in *Arabidopsis* by inhibiting the accumulation of auxin in flanking xylem-pole pericycle cells via the PIN3 and PIN7 auxin export proteins.

Keywords:
auxin maxima - auxin transport - GOLVEN - lateral roots - peptide signaling - pericycle - PIN - prebranch sites

Abstract

Lateral root initiation requires the accumulation of auxin in lateral root founder cells, yielding a local auxin maximum. The positioning of auxin maxima along the primary root determines the density and spacing of lateral roots. The GOLVEN6 (GLV6) and GLV10 signaling peptides and their receptors have been established as regulators of lateral root spacing via their inhibitory effect on lateral root initiation in *Arabidopsis*. However, it remained unclear how these GLV peptides interfere with auxin signaling or homeostasis. Here, we show that GLV6/10 signaling regulates the expression of a subset of auxin response genes, downstream of the canonical auxin signaling pathway, while simultaneously inhibiting the establishment of auxin maxima within xylem-pole pericycle cells that neighbor lateral root initiation sites. We present genetic evidence that this inhibitory effect relies on the activity of the PIN3 and PIN7 auxin export proteins. Furthermore, GLV6/10 peptide signaling was found to enhance PIN7 abundance in the plasma membranes of xylem-pole pericycle cells, which likely stimulates auxin efflux from these cells. Based on these findings, we propose a model in which the GLV6/10 signaling pathway serves as a negative feedback mechanism that contributes to the robust patterning of auxin maxima along the primary root.

Abbreviations:

a.u.	arbitrary units
ABCB	ATP-BINDING CASSETTE TYPE-B
AFB	AUXIN SIGNALING F-BOX PROTEIN
ANOVA	analysis of variance
ARF	AUXIN RESPONSE FACTOR
AUX1	AUXIN RESISTANT 1
CCD	charge-coupled device
DAG	days after germination
DIC	differential interference contrast
DMSO	dimethylsulfoxide
FC	fold change
GLV	GOLVEN
GUS	β-glucuronidase
HPLC	high performance liquid chromatography
IAA	indole-3-acetic acid
LAX	LIKE-AUX1
LBD16	LATERAL ORGAN BOUNDARIES-DOMAIN 16
LR	lateral root
LRFC	lateral root founder cell
LUC	LUCIFERASE
MS	Murashige and Skoog
MS/MS	tandem mass spectrometry
NAA	naphthaleneacetic acid
NLS	nuclear localization signal
NPA	naphthylphthalamic acid
OE	overexpression
oxIAA	2-oxindole-3-acetic acid
PIN	PIN-FORMED
PLT5	PLETHORA 5

RGI	ROOT GROWTH FACTOR INSENSITIVE
RLK	receptor-like kinase
SD	standard deviation
SE	standard error
SLR	SOLITARY ROOT
TIR1	TRANSPORT INHIBITOR RESPONSE 1
XPP	xylem-pole pericycle
YUC6	YUCCA6

Introduction

Roots enable plants to take up water and nutrients from the soil, interact with soil microbiota, and fix themselves to the substrate. Hence, a flexible root system, with the ability to branch out, is essential for the modulation of the root surface area, the exploration of different micro-environments in the soil, and the formation of a more extensive support structure. Control over the architecture of the root system is therefore of particular importance for plants, as illustrated by their ability to adjust the density and spacing of lateral roots (LRs) along the primary root based on the availability of water and nutrients, as well as the presence of certain microorganisms in the rhizosphere (López-Bucio *et al.*, 2002, 2007; Shin *et al.*, 2007; Zamioudis *et al.*, 2013; Bao *et al.*, 2014; Orman-Ligeza *et al.*, 2018; Orosa-Puente *et al.*, 2018; Kong *et al.*, 2020). Accordingly, a better understanding of the mechanisms that determine when and where LR development is initiated might enable us to make beneficial modifications to the root system architecture of certain crops through breeding efforts or biotechnological approaches. The chief regulator of LR development is the phytohormone auxin (Lavenus *et al.*, 2013; Du and Scheres, 2018). In *Arabidopsis thaliana,* LRs arise from pairs of abutting xylem-pole pericycle (XPP) cells, called lateral root founder cells (LRFCs) (Dubrovsky *et al.*, 2000, 2008; Beeckman *et al.*, 2001; Parizot *et al.*, 2008). In the young maturation zone, auxin accumulates in these cells, which can be visualized using the auxin-responsive *DR5* promoter (Ulmasov *et al.*, 1997). DR5-marked patches of XPP cells are therefore often referred to as pre-branch sites (van Norman *et al.*, 2013). Upon LR initiation, LRFCs undergo an asymmetric anticlinal cell division that is essential for further lateral root development (Malamy & Benfey, 1997; De Smet et al., 2007; De Rybel et al., 2010; Goh et al., 2012a). Extensive research has shown that the local accumulation of auxin in LRFCs and an intact auxin signaling pathway are instrumental for proper LR initiation and development. Within the LRFCs, auxin induces the breakdown of AUX/IAA proteins via TRANSPORT INHIBITOR RESPONSE 1 (TIR1) and TIR1-like AUXIN SIGNALING F-BOX PROTEINs (AFBs) (Kepinski and Leyser, 2005; Parry *et al.*, 2009), which releases AUXIN RESPONSE FACTOR (ARF) transcription factors to modulate the expression of their target genes (Ulmasov *et al.*, 1997, 1999; Gray *et al.*, 2001; Tiwari *et al.*, 2001). Several AUX/IAAs and ARFs are known to be involved in lateral root development, but IAA14/SLR, ARF7 and ARF19 seem to play the most prominent role during LR initiation (Fukaki *et al.*, 2002; Okushima *et al.*, 2005; Goh *et al.*, 2012*b*). Via this pathway, auxin modulates the expression of a host of auxin response genes that orchestrate the initiation and development of LRs (Okushima *et al.*, 2005; Vanneste *et al.*, 2005). The local auxin accumulation in LRFCs required for the induction of this pathway is achieved through careful regulation of its biosynthesis, storage and degradation (Nakazawa *et al.*, 2001; Rampey *et al.*, 2004; Ljung *et al.*, 2005; Porco *et al.*, 2016; Zhang *et al.*, 2016; Casanova-Sáez *et al.*, 2022), combined with directional auxin transport, which is mediated by 3 main classes of transmembrane transporters; the AUXIN RESISTANT 1 (AUX1) and LIKE-AUX1 (LAX) importers (Swarup and Péret, 2012), the ATP-BINDING CASSETTE TYPE-B (ABCB) exporters (Geisler *et al.*, 2017), and the PIN-FORMED (PIN) exporters (Adamowski and Friml, 2015). Defects in the auxin transport machinery can affect the spacing and density of lateral roots, and chemical inhibition of polar auxin transport can even block lateral root initiation altogether, highlighting the importance of local auxin accumulation in

LRFCs (Casimiro *et al.*, 2001; Marchant *et al.*, 2002; Benková *et al.*, 2003; Laskowski *et al.*, 2008; Mravec *et al.*, 2008; Swarup *et al.*, 2008; Marhavý *et al.*, 2013; Xuan *et al.*, 2016; Chen *et al.*, 2023).

In addition to auxin, several small secreted signaling peptides and their receptors were shown to be involved in the regulation of LR initiation and spacing (De Smet et al., 2008; Araya et al., 2014; Cho et al., 2014; Czyzewicz et al., 2015; Murphy et al., 2016; Roberts et al., 2016; Dimitrov and Tax, 2018; Dong et al., 2019; Toyokura et al., 2019; Fernandez et al., 2020; Jourquin et al., 2022). These include GOLVEN (GLV) 6 and GLV10, two members of the GOLVEN/ROOT GROWTH FACTOR/CLE-LIKE peptide family, and the receptor-like kinases (RLKs) responsible for their perception, called ROOT GROWTH FACTOR INSENSITIVE (RGI) 1-5 (Fernandez *et al.*, 2013, 2015, 2020; Ou *et al.*, 2016; Song *et al.*, 2016). *GLV6* and *GLV10* are auxin-inducible genes that start to be expressed in LRFCs right before the first asymmetric cell division that hallmarks LR initiation. They continue to be expressed throughout LR primordium development, during which their expression domains become restricted to the center of the primordium. *RGI1, 4* and *5*, are believed to be the most important receptors for GLV6/10 peptides during LR initiation (Fernandez *et al.*, 2020; Jourquin *et al.*, 2022). *RGI1* was shown to be expressed throughout the young XPP, as well as in LRFCs and young LR primordia, while its expression is mainly restricted to the flanks of the primordia during later developmental stages. *RGI5* expression is initiated in LRFCs upon LR initiation and can still be observed after the first anticlinal cell division, but is strongly reduced in later developmental stages. These expression patterns suggest that GLV6/10 peptides can be perceived by the peptide producing LRFCs themselves, as well as by the flanking pericycle cells. Overexpression (OE) or treatment with synthetic GLV6 and GLV10 peptides inhibits LR initiation and triggers aberrant anticlinal cell divisions throughout the pericycle (Meng *et al.*, 2012; Fernandez *et al.*, 2015). Conversely, double *glv6glv10* knock-out mutants were found to have increased total (non-emerged + emerged) LR primordium densities and display an irregular spacing of LR primordia along the primary root, where LR primordia often occur in pairs or clusters (Fernandez *et al.*, 2020; Jourquin *et al.*, 2022). These findings suggest that GLV6 and GLV10 peptides serve as redundantly acting inhibitors of LR initiation that regulate the spacing of LRs along the primary root. Recently, we have characterized the GLV6/10-induced transcriptional response through an RNA-sequencing experiment designed to specifically capture the effect GLV peptide signaling during LR initiation (Jourquin *et al.*, 2022). To gain a more thorough understanding of how GLV6/10 peptides regulate the spacing of LR primordia along the primary root, and given the prominent role of auxin in LR development, we set out to investigate the interplay between GLV6/10 and auxin signaling during LR initiation in more detail. Further examination of the GLV6/10-induced transcriptional response indicated that GLV6/10 peptide signaling regulates the expression of a particular subset of auxin response genes, downstream of the transcriptional auxin signaling pathway, and simultaneously attenuates the local accumulation of auxin in xylem-pole pericycle cells via the PIN3 and PIN7 auxin export proteins. The GLV6/10 signaling pathway thus constitutes a negative feedback loop on the formation of auxin maxima that ensures proper LR spacing.

Materials and Methods

Plant material and growth conditions

Unless stated otherwise, surface sterilized seeds were sown directly on solid ½ Murashige and Skoog (MS) medium (2.154g/L MS (Duchefa Biochemie), 1% sucrose, 0.1g/L Myo-inositol (Sigma-Aldrich), 0.5g/L MES (Duchefa Biochemie), 0.8% Plant Tissue Culture Agar (Lab M)). After 48h of stratification at 4°C, Petri plates were incubated at 21°C in continuous light. The following transgenic and mutant *Arabidopsis* lines were described elsewhere: *iGLV6, rgi1rgi5/iGLV6* (Fernandez *et al.*, 2020), *CYCA2;4:GUS* (Vanneste *et al.*, 2011), *CYCB1;1:GUS* (Ferreira *et al.*, 1994), *tir1-1* (Ruegger *et al.*, 1998), *afb1-3*, *afb2-3* (Savaldi-Goldstein *et al.*, 2008), *afb3-4*, *tir1-1afb2-3*, *tir1-1afb3-4* (Parry *et al.*, 2009), *arf7arf19* (Okushima *et al.*, 2005), *slr-1* (Fukaki *et al.*, 2002), *DR5:LUCIFERASE* (Moreno-Risueno *et al.*,

2010), *iGLV6/DR5:LUCIFERASE* (Fernandez *et al.*, 2020), *35S:DII-VENUS* (Vernoux *et al.*, 2011), *gh3.123456* (Porco *et al.*, 2016), *abcb1-100, abcb19-101, abcb1-100abcb19-101* (Lin and Wang, 2005), *abcb4-1* (Terasaka *et al.*, 2005), *abcb21-1* (Kamimoto *et al.*, 2012), *abcb1-100abcb19-101abcb21-1* (Jenness *et al.*, 2019), *ABCB1:ABCB1-GFP, ABCB19:ABCB19-GFP* (Mravec *et al.*, 2008), *aux1-7, AUX1:AUX1-YFP* (Swarup *et al.*, 2004), *lax1, lax2, lax3* (Swarup *et al.*, 2008), *pin1 (En134)* (Gälweiler *et al.*, 1998), *pin2 (eir1-1)*(Roman *et al.*, 1995)*, pin1pin2* (Gälweiler *et al.*, 1998), *pin3-2* (Friml *et al.*, 2002), *pin7-1* , *pin3-5pin7-1* (Benková *et al.*, 2003), *PIN3:PIN3-GFP, PIN7:PIN7-GFP* (Billou *et al.*, 2005). To generate the transcriptional *GH3* reporter lines, 2000bp promoter fragments of *GH3.1, GH3.2, GH3.3* and *GH3.5* were cloned into the pDONRP4-P1R donor vector via PB Gateway reactions. Expression clones were constructed via LR Gateway reactions in which the promoter-containing entry clones were combined with the pMK7S*NFm14GW destination vector (Karimi *et al.*, 2007). To generate the XPP specific *YUC6* overexpression line, the genomic *YUC6* sequence was cloned into the pDONR221 donor vector via a PB Gateway reaction. Expression clones were constructed via LR Gateway reactions using the pEN-L4-XPP-L1 (Andersen *et al.*, 2018), pEN-L1-YUC6-L2 and pEN-R2-GFP-L3 (Karimi *et al.*, 2007) entry clones combined with the pH7M34GW (Karimi *et al.*, 2005) destination vector. All primers used for cloning are provided in *supplementary table S1.* All resulting expression vectors were transferred to *Agrobacterium tumefaciens* strain C58C1 and transformed into wild-type *Arabidopsis thaliana* plants of the Columbia (Col-0) ecotype.

Phenotypic analyses

To assess the sensitivity of different mutant and transgenic lines to the inhibitory effect of GLV6/10 on LR initiation, Col-0 and mutant seedlings were sown on ½ MS medium and transferred to medium with or without 100 nM GLV10p at 3 days after germination (DAG). Synthetic GLV10p (DY(SO_3^-)PKPSTRPPRHN) was obtained from Genscript (>70% purity). Emerged LR numbers were counted on 12DAG seedlings using a stereo microscope. Total LR (non-emerged + emerged) numbers were quantified in 9DAG seedlings using an Olympus BX53 DIC microscope after clearing the roots as previously described (Malamy and Benfey, 1997). Scans of roots were used to measure primary root lengths with FIJI (Schindelin *et al.*, 2012; Schneider *et al.*, 2012) and densities were calculated by dividing emerged or total LR numbers by primary root lengths.
To determine whether auxin can rescue the LR inhibition caused by $GLV6^{OE}$, *iGLV6* seedlings (containing an estradiol inducible $GLV6^{OE}$ construct) were grown on plates with 2 µM estradiol, 0.1 µM 1-naphthaleneacetic acid (NAA), a combination of both, or dimethylsulfoxide (DMSO) as mock treatment. At 12DAG, emerged LR densities were quantified after which the roots were cleared as previously described (Malamy and Benfey, 1997), and imaged using an Olympus BX53 differential interference contrast (DIC) microscope to study the effects on pericycle cell divisions.
The effect of GLV10p treatment on pericycle cell divisions in *arf7arf19* mutant roots, and on the anatomy of the primary root of *abcb1abcb19* mutants, was assessed using 9DAG seedlings grown on medium with or without or 100 nM GLV10p. Similarly, the effect of $GLV6^{OE}$ on the pericycle of *slr1/iGLV6* and 10 µM naphthylphthalamic acid-treated (NPA; Duchefa Biochemie) *iGLV6* roots was assessed using 9DAG seedlings grown on medium with 2 µM estradiol (Sigma) or an equivalent volume of dimethylsulfoxide (DMSO). Seedlings were fixed and cleared using the ClearSee protocol (Kurihara *et al.*, 2015; Ursache *et al.*, 2018) and cell walls were stained using Calcofluor White (Sigma). Images were taken using a Zeiss LSM710 confocal microscope. Calcofluor White was excited at 405 nm and acquired at 430-470 nm.

Expression pattern analyses

To assess the effect of GLV6/10 on *CYCA2;4* and *CYCB1;1* expression, *CYCA2;4:GUS* seedlings were grown on medium with or without 200 nM GLV10p, while *CYCB1;1:GUS* and *CYCB1;1:GUS/35S-GLV6* seedlings were all grown on standard ½ MS medium. Seedlings were collected for GUS (β-glucuronidase) staining at 9DAG. To assess the effect of GLV10p treatment on *GH3.1, GH3.2, GH3.3* and *GH3.5* expression, *GH3.1:NLS-GFP-GUS, GH3.2:NLS-GFP-GUS, GH3.3:NLS-GFP-GUS* and

GH3.5:NLS-GFP-GUS seedlings were grown on ½ MS medium for 4 days, after which they were transferred to medium with or without 1 µM GLV10p and gravistimulated to induce LR initiation. 18 hours after gravistimulation, seedlings were collected for GUS staining. GUS staining was performed as previously described after fixation in 90% acetone at 4°C (Beeckman and Engler, 1994). Images were taken with an Olympus BX53 DIC microscope or a KEYENCE VHX-7000 digital microscope.
All confocal images were taken using a Zeiss LSM710 microscope. GFP was excited at 488 nm and acquired at 495-540 nm. YFP and VENUS were excited at 514 nm and acquired at 515-555 nm. To analyze the effect of GLV10p on fluorescent reporter lines (*35S:DII-VENUS, ABCB1:ABCB1-GFP, ABCB19:ABCB19-GFP, AUX1:AUX1-YFP, PIN3:PIN3-GFP* and *PIN7:PIN7-GFP*) during LR initiation, seedlings were gravistimulated (90° counter clockwise rotation) at 4DAG, and 8h later, transferred to medium with or without1 µM GLV10p. Root bends, older parts of the maturation zone, and root tips, were imaged 10h after peptide treatment (= 18h after gravistimulation). For measurements of PIN3-GFP and PIN7-GFP intensity, *PIN3:PIN3-GFP* and *PIN7:PIN7-GFP* seedlings were transferred to medium with or without 1 µM GLV10p at 8DAG. At 9DAG, confocal images were taken in the young maturation zone (from the start of the maturation zone up to the first stage II primordium) of 15 seedlings per condition. For every seedling, the mean fluorescence intensity of the PIN3-GFP or PIN7-GFP signal was quantified in three anticlinal xylem-pole pericycle cell membranes using FIJI (Schindelin *et al.*, 2012; Schneider *et al.*, 2012).

HPLC-MS/MS based profiling of auxin levels

Seedlings of the *iGLV6* line were grown on nylon membranes with a 20 µm mesh size (Prosep) placed on top of standard ½MS medium for 4 days, after which they were gravistimulated (90° counterclockwise rotation). 8h after gravistimulation, seedlings were transferred to medium containing 2 µM estradiol or an equivalent volume of DMSO. 12h and 24h after transfer, 100 root bends were dissected and collected per sample. 5 biological replicates were obtained for each condition. The extraction, purification and the LC-MS analysis of endogenous indole-3-acetic acid (IAA) and its metabolites and amino acid conjugates was carried out according to (Novák *et al.*, 2012) with some modification to also include jasmonic acid + amino acid conjugates (data not shown). Briefly, 100 root bends per sample were homogenized using a bead mill (27Hz, 10min, 4°C; MixerMill, Retsch GmbH, Haan, Germany) and extracted in 1ml of 50 mM sodium phosphate buffer containing 1% sodium diethyldithiocarbamate and a mixture of 13C6- or deuterium-labelled internal standards. After centrifugation (14000 RPM, 15min, 4°C), the supernatant was immediately processed as follows. Sample pH was adjusted to 2.5 using 1M HCl. Samples were applied to preconditioned Oasis HLB solid-phase extraction columns (30 mg 1 cc, Waters Inc., Milford, MA, USA). After sample application, columns were rinsed with 2ml 5% methanol. Compounds of interest were then eluted with 2ml 80% methanol. Mass spectrometry analysis and quantification were performed using an LC-MS/MS system comprised of a 1290 Infinity Binary LC System coupled to a 6495 Triple Quad LC/MS System with Jet Stream and Dual Ion Funnel technologies (Agilent Technologies, Santa Clara, CA, USA).

DR5:LUCIFERASE imaging

To count the number of *DR5:LUCIFERASE* (*DR5:LUC*) sites per root, 9DAG *DR5:LUC* and *gh3.123456* x *DR5:LUC* seedlings were sprayed with 1 mM D-Luciferin (Duchefa Biochemie) solution [D-Luciferin dissolved in 0.01% (v/v) Tween80 and 0.1% (v/v) DMSO] and kept in total darkness for 10min before imaging. To quantify the effect of GLV10p treatment on *DR5:LUCIFERASE* expression in *abcb1abcb19* mutants during LR initiation, 4 day old *DR5:LUC* and *abcb1abcb19* x *DR5:LUC* seedlings were transferred medium with or without 1 µM GLV10p and gravistimulated (90° counter clockwise rotation). 24h later, seedlings were sprayed with 1 mM D-Luciferin solution and kept in total darkness for 10min before imaging. Emitted LUCIFERASE signal was captured using an ANDOR iKon-M 934 charge-coupled device (CCD) camera (Oxford Instruments) paired with a fixed lens (Spacecom 43F2409M-MP C 4/3'' 24 mm F0.9) over a 20min exposure time. If required, corresponding brightfield images were taken to measure the primary root lengths with FIJI (Schindelin *et al.*, 2012; Schneider *et*

al., 2012) and densities were calculated by dividing DR5:LUC site numbers by primary root lengths. For time-lapse imaging of *DR5*:*LUC* expression in gravistimulation-induced root bends, 4DAG *DR5:LUC/iGLV6* seedlings were gravistimulated (90° counter clockwise rotation), and 8h later, transferred to medium containing 2 µM estradiol or DMSO, after which they were immediately prepared for imaging. For the comparative time lapse imaging of *DR5:LUC* expression in peptide treated wild-type and *gh3.123456* backgrounds, 5DAG *DR5:LUC* and *gh3.123456/DR5:LUC* seedlings were transferred to medium with or without 1 µM GLV10p, and immediately prepared for imaging. Seedlings were sprayed with 1 mM D-Luciferin solution and kept in total darkness for 10min before initiating the time course. Emitted LUCIFERASE signal was captured using a NightSHADE LB985 in vivo plant imaging system (Berthold technologies) equipped with a deep-cooled slow scan CCD camera and the accompanying lens (Andor Instruments). An image was taken every 20min with a 10min exposure time. Measurement of signal intensities in the root bends and the generation of kymographs was performed using Fiji.

RT-qPCR experiments

Roots were sampled from 7DAG Col-0 and *arf7arf19* seedlings that were incubated for 24h in liquid ½MS, with or without 1 µM GLV10p. Total RNA was isolated using the ReliaPrep™ RNA Miniprep System (Promega). cDNA was synthesized with the qScript® cDNA SuperMix (Quantabio). RT-qPCRs were performed using SYBR® Green Mix (Roche) in a LightCycler® 480 (Roche). *CKA2* and *CDKA1* were included as housekeeping genes. Used primers are provided in *supplementary table S1.*

Gene Ontology enrichment analyses

Overrepresented gene ontology (GO) terms for biological processes, as defined by the PANTHER classification system (Mi *et al.*, 2019), were performed via a Fisher's exact test with Bonferroni correction using the PANTHER GO tool (www.pantherdb.org).

Statistical analyses

Statistical analyses were performed in R (R Core Team, 2020). For LR and DR5:LUC site density data, a Poisson model (or a quasipoisson model in case of over- or under-dispersion) was fitted to the LR or DR5:LUC site counts, with treatment, genotype, and their interaction as fixed effects. A log-link function was applied, and log-transformed primary root lengths were used as an offset variable. Statistical analysis of primary root lengths was performed via a two-way analysis of variance (ANOVA) with treatment, genotype, and their interaction as fixed effects. Contrasts and post-hoc interaction analyses were set up using the “emmeans” or the “phia” package (De Rosario-Martinez, 2015; Lenth, 2021) and a Dunnett correction was implemented where applicable. *DR5:LUC* intensity measurements in untreated and GLV10p-treated root bends of wild-type and *abcb1abcb19* seedlings were compared via a two-way ANOVA with genotype and treatment as fixed effects, followed by a post-hoc Tukey test. Fluorescence intensity measurements were compared via a Mann-Whitney test. For the statistical analysis of RT-qPCR data, log2 fold changes in expression levels between treatment and mock conditions were calculated for each genotype, and two-tailed Student’s t-tests were performed to compare treatment effects between genotypes. Statistical significance of the GLV10p-induced changes of the proportions of *GUS*-expressing and non *GUS*-expressing *GH3*:GUS seedlings was determined via Fisher’s exact tests. The levels of free IAA and its derivatives were compared via two-way ANOVA with treatment and time as fixed effects, followed by post-hoc Tukey tests. For the pairwise comparison of transcriptomic datasets, the probability of finding the observed number of overlapping genes was determined using a hypergeometric test. Note that only genes for which reads/hits could be detected in all experiments were included in the analysis to mediate biased results due to differences in the sampling procedures (e.g. genes expressed specifically in the root tip were excluded since they are not detected in the $GLV6^{OE}$ dataset).

Results

GLV6/10 signaling regulates a subset of auxin response genes downstream of the canonical auxin signaling pathway

We previously identified a set of about 800 genes that are differentially regulated upon *GLV6* overexpression (OE) during LR initiation via an RNA-sequencing experiment using an estradiol-inducible *GLV6*^{OE} line (*iGLV6*) in combination with gravistimulation-induced LR initiation (Jourquin *et al.*, 2022). In agreement with the regulatory role for GLV6/10 peptides during LR initiation, GO-enrichment analysis on these GLV response genes revealed an enrichment for genes associated with LR formation and root system architecture, as well as auxin responses and transport (Supplementary Fig. S1). Indeed, the previously established target genes of the GLV6/10-RGI module, *PUCHI, PLETHORA 5* (*PLT5*) and LATERAL ORGAN BOUNDARIES-DOMAIN 16 (*LBD16*), are all known to be auxin inducible (Hirota *et al.*, 2007; Okushima *et al.*, 2007; Hofhuis *et al.*, 2013). Comparative analysis of the GLV6-induced transcriptional response with previously reported transcriptomic effects of NAA and IAA treatment on *Arabidopsis* roots (Okushima *et al.*, 2005; Vanneste *et al.*, 2005) revealed that nearly all GLV6-regulated genes are also regulated by auxin in a SLR/IAA14 and ARF7/19 dependent manner (Fig. 1A). More precisely, most GLV6-induced genes are also induced by auxin, while the large majority of genes downregulated by GLV6 are downregulated by auxin as well (Supplementary Fig. S2, Supplementary Table S2). This large overlap between GLV6 and auxin response genes, prompted us to investigate whether GLV6/10 peptides establish their effects via auxin. When grown in the presence of GLV10p, mutants in the auxin receptor TRANSPORT INHIBITOR RESPONSE 1 (TIR1), or its homologous AUXIN SIGNALING F-BOX PROTEINS (AFBs) (Parry *et al.*, 2009), showed a similar percentual decrease in emerged LR density compared to wild-type seedlings (Fig. 1B), suggesting that the perception of auxin is not necessary for the inhibitory effect of GLVs on LR initiation. Auxin largely regulates LR development via the ARF7 and ARF19 transcription factors, and their negative regulator SLR/IAA14 (Fukaki *et al.*, 2002; Okushima *et al.*, 2005). Since *arf7arf19,* as well as the dominant negative *slr-1* mutants, do not produce LR primordia, the effect of GLV10p treatment or *GLV6*^{OE} on these mutants was assessed through microscopic analysis of the pericycle. This revealed that both mutants still show the ectopic anticlinal pericycle cell divisions typically observed in the presence of an excess of GLV6/10 peptides (Fig. 1C). Furthermore, such ectopic anticlinal pericycle divisions can also still be induced upon *GLV6*^{OE} in the presence of the auxin transport inhibitor NPA (Fig. 1C), which typically inhibits LR initiation by preventing auxin accumulation in LRFCs (Casimiro *et al.*, 2001). These data thus indicate that the effect of GLV peptides on pericycle cell divisions does not require auxin transport or signaling. In agreement with this, RT-qPCR analysis of a set of GLV6/10 response genes indicated that their response to GLV10p treatment is not attenuated in the *arf7arf19* mutant background (Fig. 1D). Combined with the fact that expression of *GLV6* and *GLV10* is known to be auxin inducible via ARF7/19 and their downstream target LBD16 (Fernandez *et al.*, 2020; Jourquin *et al.*, 2022), this suggests that these GLV peptides are involved in the regulation of a part of the transcriptional auxin response, downstream of the core auxin signaling machinery that controls LR initiation.

The overlapping GLV- and auxin-induced transcriptional responses seem somewhat counterintuitive, since auxin treatments typically trigger formative divisions throughout the xylem-pole pericycle, resulting in the formation of many LRs along the whole primary root (Parizot *et al.*, 2008), while GLV6/10 peptides inhibit LR initiation. However, an excess of GLV6/10 peptides does not merely inhibit the first asymmetric cell divisions of LRFCs. Rather, as evidenced by the long stretches of short pericycle cells observed in peptide-treated roots, an overabundance of GLV6/10 peptides triggers ectopic anticlinal cell divisions throughout the pericycle (Fig. 1C)(Meng *et al.*, 2012; Fernandez *et al.*, 2015, 2020). In agreement with this, the late transcriptional response to *GLV6*^{OE} (6h after induction) is enriched for genes involved in the regulation of cell division (Supplementary Fig. S3). The cell-cycle gene that was most strongly induced after *GLV6*^{OE} was *CYCA2;4*, and analysis of a *CYCA2;4:GUS* reporter line revealed that it is ectopically expressed along the whole pericycle after treatment with GLV10p, as opposed to its typical association with sites of LR development in untreated conditions (Fig.

2A, 2B) (Vanneste *et al.*, 2011). In contrast, the cell cycle gene *CYCB1;1,* which typically marks the formative pericycle cell divisions of LR founder cells and LR primordia, and which is known to be induced throughout the pericycle upon auxin treatment (Himanen *et al.*, 2002), did not respond to *GLV6^{OE}* in our RNA-sequencing experiment, nor could any *CYCB1;1:GUS* activity be observed in the pericycle of *GLV6* overexpressing plants (Fig. 2C). Despite the overlapping transcriptional responses, there thus seems to be an important difference between the pericycle divisions triggered by auxin, which are formative and lead to the development of LR primordia, and the divisions triggered by an excess of GLV6/10 peptides, which do not give rise to LR primordia. In this context, it should be noted that the GLV6 response genes constitute only a fraction of the complete auxin response that was characterized through prior transcriptome analyses in the root (Fig. 1A), indicating that *GLV6^{OE}* only triggers a partial auxin response. This GLV-induced partial auxin response thus seems to stimulate pericycle cell divisions, but is not sufficient for the proper initiation of LR development.

GLV6/10 overabundance disrupts the auxin accumulation in LRFCs required for lateral root initiation

Given the opposing effects of GLV6/10 and auxin on LR initiation, despite their overlapping transcriptional effects, we investigated the impact of ectopic GLV6/10 signaling on auxin signaling and homeostasis during LR initiation. Our previous analysis of the expression of the auxin-responsive *DR5* promoter suggested that *GLV6^{OE}* attenuates auxin signaling activity in pre-branch sites (Fernandez *et al.*, 2020). A more thorough analysis indeed revealed that, when *GLV6^{OE}* is induced 8 hours after gravistimulation (± 4h prior to LR initiation (Jourquin *et al.*, 2022)), the *DR5:LUCIFERASE* (*DR5:LUC*) signal in the gravistimulation-induced pre-branch site is gradually reduced, while a clear pre-branch site with high *DR5:LUC* intensity is typically established and maintained in the root bends of untreated seedlings (Fig. 3A, 3B). *GLV6^{OE}* thus seems to abolish pre-branch site formation completely. Additionally, expression of the *35S:DII-VENUS* reporter was analyzed upon GLV10p treatment after gravistimulation-induced LR initiation. The fusion of VENUS to the degron domain of an AUX/IAA protein (DII) renders it susceptible to auxin-induced degradation via interaction with TIR1/AFB proteins, making its fluorescence intensity inversely correlated to endogenous auxin levels (Vernoux *et al.*, 2011). In the absence of synthetic GLV10p, only a very faint DII-VENUS signal could be observed in the pericycle after gravistimulation-induced LR initiation, while a clear nuclear DII-VENUS signal was detected in pericycle cells of GLV10p-treated seedlings (Fig. 3C). Hence, these data imply that *GLV6^{OE}* and GLV10p treatments disrupt the accumulation of auxin in LRFCs, thereby preventing LR initiation.

Exploring the effect of GLV6/10 peptide signaling on auxin metabolism during lateral root initiation

The set of GLV6 response genes, identified through the *GLV6^{OE}* RNA-sequencing experiment, contains several genes involved in auxin metabolism and transport that might be responsible for the disruption of auxin accumulation in LRFCs when GLV6/10 peptides are in overabundance (Jourquin *et al.*, 2022). This includes four GH3 encoding genes (*GH3.1, GH3.2, GH3.3* and *GH3.5*), which were all found to be downregulated upon *GLV6^{OE}* in an RGI-dependent manner (Supplementary Fig. S4). This suppression was confirmed using *GH3:GUS* reporter lines that were gravistimulated and treated with GLV10p (Fig. 4A). While transcription of each of these *GH3s* could typically be detected upon LR initiation (18h after gravistimulation) in untreated conditions, their expression was found to be lacking in the root bends of most GLV10p-treated seedlings (Fig. 4A, Supplementary Fig. S5). These *GH3s* are among the few genes that show opposing responses to *GLV6^{OE}* and auxin treatment (Supplementary Table S2), since they are typically induced by auxin rather than suppressed (Hagen and Guilfoyle, 2002; Okushima *et al.*, 2005). As members of the group II GH3s, they function as enzymes that catalyze the conjugation of free IAA to amino acids (AAs) (Staswick *et al.*, 2002, 2005). These IAA-AA conjugates are believed to serve as inactive storage forms of auxin and/or intermediates in the auxin degradation pathway (Ludwig-Müller, 2011; Hayashi *et al.*, 2021; Casanova-Sáez *et al.*, 2022). The downregulation of *GH3s*

through GLV peptide signaling can thus not account for a reduction in auxin levels, but we hypothesized that GH3 enzymes might be post-translationally activated through GLV-RGI signaling. To assess the importance of GH3s for the effect of GLV6/10 on the accumulation of auxin in LRFCs, we made use of a *gh3.123456* sextuple mutant (Porco *et al.*, 2016). In agreement with the auxin conjugating activity of GH3.1-6, the *gh3.123456* mutant was previously shown to contain increased levels of free auxin and displayed a higher emerged LR density compared to wild-type seedlings (Porco *et al.*, 2016). Interestingly, the GLV10p-triggered reductions in emerged, as well as total LR densities, were significantly less severe in *gh3.123456* mutants than in wild-type plants (Fig. 4B, Supplementary Fig. S6). Furthermore, we analyzed *DR5:LUC* expression in wild-type and *gh3.123456* mutant backgrounds when grown in the presence of GLV10p. As with *GLV6*^{OE}, high concentrations of GLV10p largely inhibited the establishment of pre-branch sites and could even reduce the DR5:LUC activity in pre-branch sites that were established before treatment. In *gh3.123456* mutants on the other hand, pre-branch sites with clear *DR5:LUC* expression could still be established after GLV10p treatment (Fig. 4C, Supplementary Fig. S7). In agreement with this, *gh3.123456* mutant seedlings grown in the presence of GLV10p showed a significantly less pronounced reduction in *DR5:LUC* site density compared to wild-type seedlings (Supplementary Fig. S8). It is possible that the increased auxin level in *gh3.123456* mutants (Porco *et al.*, 2016) dampens the effect of GLV10p treatment, even if GH3s are not directly involved. Indeed, we found that exogenous auxin treatments can partially overcome the inhibitory effect of GLV6/10 signaling on LR initiation. Emerged LR densities were quantified upon estradiol-induced *GLV6*^{OE}, combined with treatments with the synthetic auxin analog NAA (Fig. 4D). The high LR densities typically observed in the presence of NAA were clearly reduced upon *GLV6*^{OE}, but were still high compared to the nearly complete inhibition of LR development observed when *GLV6* is overexpressed in the absence of NAA. Additionally, auxin levels can be ectopically increased specifically in the XPP, via the tissue specific expression of *YUCCA6* (*YUC6*), encoding one of the YUCCA enzymes that catalyze a rate-limiting step in IAA biosynthesis (Zhao *et al.*, 2001). This also resulted in a strong increase in emerged LR density, which could only be reduced weakly upon treatment with GLV10p compared to the reduction observed in wild-type seedlings (Fig. 4E). Importantly, microscopic analysis of NAA-treated roots showed that the pericycle cells in-between LR primordia still undergo many ectopic cell divisions when *GLV6* is being overexpressed, while the LR primordia in roots treated with NAA alone are flanked by pericycle cells that are long and narrow as observed in untreated conditions (Fig. 4F). This suggests that increased auxin levels do not inhibit the occurrence of GLV6/10-induced ectopic pericycle cell divisions, but rather overrule the inhibitory effect on LR initiation, possibly by compensating for the GLV6/10-induced lack of auxin in LRFCs.

To unambiguously determine whether GLV6/10 peptide signaling might regulate free auxin levels during LR initiation, the effect of GLV peptide signaling on the levels of free IAA, as well as its conjugates and breakdown products was determined after gravistimulation-induced LR initiation. To this end, *iGLV6* seedlings were treated with estradiol 8 hours after gravistimulation, and root bends were sampled 12h and 24h after treatment, time points at which the *DR5:LUC* signal in the root bends was shown to be clearly reduced or had disappeared altogether (Fig. 3A, 3B). The HPLC-MS/MS based profiling of free IAA and its derivatives allowed for the detection of IAA itself, its inactive breakdown product oxIAA, both of their conjugates to glucose, and to the two IAA-AA conjugates, IAA-Aspartate and IAA-Glutamate. Other IAA-AA conjugates could not be detected, but as IAA-Aspartate and IAA-Glutamate are the main IAA-AA conjugates that are produced by GH3s *in planta,* changes in their levels can be expected if the activity or abundance of GH3 enzymes would be modulated (Staswick *et al.*, 2005; Park *et al.*, 2007; Mellor *et al.*, 2016; Porco *et al.*, 2016). However, we could not detect significant changes in free IAA levels, nor in the levels of any of its derivatives or conjugates, in *GLV6* overexpressing compared to the corresponding mock treated root bends (Fig. 4G). Free auxin levels within the sampled root bends thus appear to be unaffected when *GLV6* is overexpressed. The GLV6/10-induced reduction of *DR5:LUC* activity in pre-branch sites is therefore likely caused by a failure to concentrate the available auxin in LRFCs, rather than by an effect auxin metabolism.

GLV6/10 signaling affects auxin transport during lateral root initiation via PIN auxin exporters

The inhibitory effect of GLV6/10 peptide signaling on the establishment of an auxin maximum in LRFCs might thus result from a disruption of auxin transport rather than from an effect on auxin metabolism. The genes encoding the auxin exporters ATP-BINDING CASETTE TYPE-B 19 (ABCB19) and ABCB21 (Geisler *et al.*, 2005; Kamimoto *et al.*, 2012) were found to be upregulated upon *GLV6^{OE}* (Supplementary Fig. S4), suggesting that they might be involved in the effect of GLV6/10 peptides on auxin distribution. To assess whether these ABCBs indeed play a role in GLV6/10 peptide signaling during LR initiation, the effect of GLV10p treatment on root architecture was determined in single and higher order mutants of *ABCB19, ABCB21*, and their closest homologs *ABCB1* and *ABCB4,* respectively. Most mutants showed a GLV10p-induced decrease in emerged LR density comparable to wild-type seedlings (Fig. 5A), as well as a slight increase in primary root length typically observed upon GLV10p treatment or *GLV6^{OE}* (Supplementary Fig. S9). However, *abcb1abcb19* and *abcb1abcb19abcb21* mutants showed a striking decrease in primary root length upon GLV10p treatment (Fig. 5B, Supplementary Fig. S9), to such an extent that a reliable analysis of LR densities was not possible. Microscopic analysis revealed that GLV10p treatment on *abcb1abcb19* mutants caused extremely disorganized divisions throughout the maturation zone, not only in the pericycle, but also in endodermal, cortical and epidermal cells, and possibly also in the vasculature (Supplementary Fig. S10). The extreme response of seedlings that are defective in both *ABCB1* and *ABCB19* indicates that the combined effect of these mutations and excessive GLV peptide signaling on auxin transport results in a strong disruption of primary root development. However, this is a rather slow effect, since primary root growth did not seem to be affected within the first 24h after treatment, allowing for the study of pre-branch site formation after gravistimulation. *DR5:LUC* expression was quantified in the root bends of *abcb1abcb19* mutants 24h after gravistimulation and GLV10p treatment (Fig. 5C, 5D). The clear GLV10p-induced suppression of *DR5:LUC* expression in the *abcb1abcb19* mutant, similar to the suppression observed in the wild-type background, indicates that ABCB1 and ABCB19 are not required for the inhibitory effect of GLV6/10 peptides on local auxin accumulation. Additionally, treatment with GLV10p did not cause any obvious changes in the *ABCB1:ABCB1-GFP* and *ABCB19:ABCB19-GFP* expression patterns (Supplementary Fig. S11). These data indicate that ABCB1 and ABCB19 are not required for the inhibition of pre-branch site establishment upon superfluous GLV6/10 signaling.

To further examine the link between GLV6/10 peptide signaling and auxin transport, the effect of GLV10p treatment on LR development was analyzed in several other mutants for known auxin transporters. None of these mutants displayed the severe primary root growth defects observed in peptide-treated *abcb1abcb19* mutants (Supplementary Fig. S12). However, mutants in the auxin importer AUXIN RESISTANT 1 (AUX1) (Marchant *et al.*, 2002; Yang *et al.*, 2006) showed a stronger GLV10p-induced decrease in emerged LR density compared to wild-type seedlings, suggesting that these mutants are more responsive to peptide treatment (Fig. 6A). Conversely, double mutants in the closely related PIN-FORMED 3 (PIN3) and PIN7 auxin exporters were found to be almost completely resistant to the inhibitory effect of GLV10p treatment on LR initiation, suggesting that GLV6/10 peptides exert their effect on auxin transport via these PIN proteins (Fig. 6A). The expression patterns of some of these transporters also seemed to be affected upon GLV10p treatment (Fig 6B, Supplementary Fig. S13). Throughout the maturation zone of the primary root, weak *AUX1:AUX1-YFP* expression could be detected in the vasculature, but a clear signal was detected in LRFCs and developing LR primordia (Marchant *et al.*, 2002; Laskowski *et al.*, 2008). In the presence of GLV10p however, AUX1-YFP signal was found throughout large parts of the pericycle, in which ectopic anticlinal divisions could often be observed (Fig. 6B). Strong expression of *PIN3:PIN3-GFP* and *PIN7:PIN7-GFP* reporters was observed in the vasculature, and clear but weaker PIN3-GFP and PIN7-GFP signals were also consistently detected throughout the pericycle, which became stronger after LR initiation (Billou *et al.*, 2005). An obvious and consistent effect of GLV10p treatment on *PIN3:PIN3-GFP* expression could not be discerned, but a brighter PIN7-GFP signal was observed along large parts of the pericycle, again

often in association with GLV10p-induced ectopic anticlinal cell divisions (Supplementary Fig. S13). To corroborate this, the effect of GLV10p treatment on *PIN3:PIN3-GFP* and *PIN7:PIN7-GFP* fluorescence intensity was quantified in anticlinal membranes of xylem-pole pericycle cells within the young maturation zone (Fig. 6C, 6D). GLV-induced changes in *PIN3-GFP* fluorescence intensity could be detected, but a significant increase in PIN7-GFP fluorescence intensity was recorded upon GLV10p treatment, indicating that GLV6/10 signaling enhances PIN7 abundance in the plasma membrane of xylem-pole pericycle cells. The effect of GLV6/10-RGI signaling on auxin fluxes during LR initiation is therefore likely established via the modulation of PIN7 levels in XPP and LR founder cells.

Discussion

Previous research established the GLV6 and GLV10 signaling peptides as redundantly acting inhibitors of LR initiation (Fernandez *et al.*, 2015, 2020). Knocking out both *GLV6* and *GLV10* leads to an increase in LR initiation events and an aberrant spacing of LR primordia, while an excess of GLV6 or GLV10 peptides results in a strong decrease in LR primordium density. The latter inhibitory effect was found to be associated with the occurrence of ectopic, and relatively symmetric, anticlinal cell divisions throughout the pericycle (Meng *et al.*, 2012; Fernandez *et al.*, 2015; Jourquin *et al.*, 2022). This indicates that these peptides do not merely inhibit LRFC divisions, but somehow stimulate non-formative pericycle cell divisions. In agreement with this, we found that GLV6/10 peptides do not directly inhibit the expression of key regulators of LR initiation, but actually trigger an auxin-like response in their target cells (i.e. pericycle cells, including LRFCs). Our data indicate that this partial auxin response and the ectopic pericycle cell divisions do not rely on auxin perception or signaling. As the transcription of the *GLV6* and *GLV10* genes themselves is auxin inducible (Fernandez *et al.*, 2020; Jourquin *et al.*, 2022), this suggests that these peptides aid in the regulation of a subset of auxin response genes, downstream of the canonical auxin signaling pathway, which includes several cell cycle genes. This GLV-induced partial auxin response is thus likely the cause of the ectopic anticlinal pericycle cell divisions observed when GLV6/10 peptides are in excess, but does not readily explain how these peptides inhibit LR initiation. Interestingly, despite this auxin-like transcriptional response, we found that auxin itself fails to accumulate in LRFCs upon $GLV6^{OE}$ or GLV10p treatment. Hence, we propose that the inhibitory effect of GLV6/10 signaling on LR initiation is caused by the absence of sufficiently high auxin levels and the associated lack of a full transcriptional auxin response in LRFCs.

Initially, we investigated whether the GLV6/10-induced inhibition of pre-branch site establishment might result from an effect on auxin metabolism, since several group II *GH3* genes were differentially regulated upon $GLV6^{OE}$. We initially hypothesized that GLV6/10 peptide signaling might stimulate IAA-AA conjugation via these GH3 enzymes, thereby reducing the levels of free auxin in LRFCs. In agreement with this, overexpression and dominant gain-of-function mutants of several *GH3* genes were reported to show strong reductions in emerged LR densities, while *gh3.123456* sextuple mutants were found to have an increased LR density, phenotypes that correspond to those of $GLV6^{OE}$ lines and *glv6glv10* double mutants, respectively (Nakazawa *et al.*, 2001; Takase *et al.*, 2004; Xuan *et al.*, 2015; Porco *et al.*, 2016). Furthermore, *gh3.123456* mutants were found to be somewhat resistant to the effects of GLV10p treatments on auxin distribution and LR initiation. However, despite the clear disappearance of *DR5:LUC*-marked pre-branch sites, the levels of free IAA and its detectable conjugates and degradation products were found to be unaffected in root bends of *GLV6* overexpressing seedlings. These data thus indicate that $GLV6^{OE}$ does not affect overall IAA levels in the root, but rather prevents its accumulation in LRFCs. This is likely the result of an effect on auxin transport, rather than on auxin conjugation or degradation. The GLV6-induced downregulation of *GH3.1, GH3.2, GH3.3* and *GH3.5* expression, which drew our attention to these genes in the first place, might actually be a result of the reduced auxin levels in pre-branch sites, rather than a direct response to GLV6/10 signaling. Transcription of these *GH3* genes is known to respond extremely quickly to even relatively small changes in auxin concentrations (Paponov *et al.*, 2008). This could explain why these *GH3s* are among the very limited number of genes that show opposing responses to $GLV6^{OE}$ and auxin

treatment. We found that exogenous NAA treatments, as well as the stimulation of IAA production specifically in the XPP, also resulted in a reduced inhibitory effect of GLV6/10 peptides on LR initiation. Therefore, the hyposensitivity of *gh3.123456* mutants to GLV10p treatment likely results from the increased IAA levels in these mutants (Porco *et al.*, 2016).

Since auxin metabolism seemed to be unaffected by GLV6/10 peptide signaling, we investigated whether these peptides might influence LR initiation via an effect on auxin transport. Mutants in members of several classes of auxin transport proteins were found to show aberrant responses to GLV10p treatment, pointing to a connection between GLV6/10 signaling and auxin transport. The *ABCB1, ABCB4, ABCB19* and *ABCB21* auxin exporters are all known to be implicated in LR development (Noh *et al.*, 2001; Lin and Wang, 2005; Santelia *et al.*, 2005; Wu *et al.*, 2007; Jenness *et al.*, 2019). Interestingly, strong primary root growth defects were observed in GLV10p-treated *abcb1abcb19* mutants. This suggests that the combined effect of superfluous GLV6/10 signaling with these mutations disorganizes the distribution of auxin to such an extent that root development is severely disrupted. However, the lack of GLV10p-induced changes in *ABCB1:ABCB1-GFP* and *ABCB19:ABCB19-GFP* expression patterns, and the clear suppression of pre-branch site establishment upon GLV10p treatment of *abcb1abcb19* mutant roots, indicates that these ABCBs are not required for the response to GLV6/10 peptides. Similarly, the increased responsivity of *aux1* mutants to GLV10p-induced inhibition of LR initiation suggests that AUX1 activity antagonizes GLV6/10-RGI signaling. This is indeed plausible, as AUX1-mediated auxin import into LRFCs is known to enhance local auxin accumulation, which likely opposes the effect of GLV6/10 peptides (Marchant *et al.*, 2002; Laskowski *et al.*, 2008). The misexpression of AUX1 throughout large stretches of the pericycle is therefore unlikely to be the cause of the GLV10p-induced LR initiation defects. The PIN3 and PIN7 auxin export proteins on the other hand, seem to be imperative for the effect of GLV6/10 signaling on LR initiation, since *pin3pin7* double mutants displayed an almost complete resistance to GLV10p treatment. This behavior was not observed in *pin3* and *pin7* single mutants, in agreement with previous reports showing that both of these auxin exporters act redundantly in several processes (Kleine-Vehn *et al.*, 2010; Lewis *et al.*, 2011; Marhavý *et al.*, 2013; Wang *et al.*, 2015). The inhibitory effect of GLV6/10 signaling on the establishment of auxin maxima in LRFCs is thus likely achieved via the PIN3 and PIN7 auxin exporters. GLV10p treatment did not trigger any measurable changes in *PIN3:PIN3-GFP* expression, but resulted in a stronger expression of *PIN7:PIN7-GFP* throughout the pericycle, with significantly increased PIN7-GFP levels in anticlinal membranes of xylem-pole pericycle cells. GLV6/10 signaling might thus stimulate auxin export from its target cells by increasing PIN7 abundance. In agreement with this, ethylene-induced increases in *PIN3* and *PIN7* expression, as well as cytokinin-induced transcriptional activation of *PIN7,* were previously shown to result in an inhibition of LR initiation (Lewis *et al.*, 2011; Šimášková *et al.*, 2015), and *pin3pin7* double mutants are known to show defects in LR spacing (Benková *et al.*, 2003; Laskowski *et al.*, 2008). Additionally, previous research has indicated that GLV peptide signaling can enhance PIN2 levels in the plasma membranes of epidermal and cortical cells in the root apical meristem, which in turn affects gravitropic root growth (Whitford *et al.*, 2012). Although our data do not point to the involvement of PIN2 in the GLV6/10-RGI pathway during LR initiation, the modulation of PIN abundance in the plasma membrane via GLV signaling might be a general mechanism. The effect of GLV6/10 signaling on PIN7 abundance might be at least partially transcriptional, since *PIN7* expression was found to be significantly upregulated upon *GLV6*^{OE}, albeit with a very low fold change (FC=1.2) (Supplementary table S2). However, in light of the recently observed stimulation of PIN2 phosphorylation upon GLV peptide signaling, post-translational effects of GLV6/10 signaling on PIN3 and PIN7 abundance and activity are also very likely (Xu *et al.,* 2023).

Although further research is required to elucidate the exact molecular mechanism via which GLV6/10 peptides affect PIN plasma membrane abundance and auxin transport, the results presented here allow us to formulate a model for how the cross-talk between auxin and GLV6/10-RGI signaling controls LR spacing and development (Fig. 7). LRFCs are believed to be primed for LR formation by recurrent peaks of auxin signaling activity in the elongation zone, the frequency of which largely determines the

distance between consecutive LRs (De Smet et al., 2007; Moreno-Risueno et al., 2010; Xuan et al., 2015). However, it has been shown that, even in wild-type seedlings, multiple pairs of LRFCs are often specified in close proximity to one another, but that typically only one pair will give rise to a primordium, indicating that the others are somehow suppressed (Toyokura *et al.*, 2019). The TARGET OF LBD SIXTEEN 2 (TOLS2) peptide and its receptor RLK7 were found to be involved in this process, and we believe that GLV6/10-RGI signaling plays a similar role. Auxin is well known for its ability to regulate its own distribution via feedback loops on its biosynthesis and degradation, as well as its intercellular transport, typically generating well defined and regularly spaced auxin maxima in both the shoot and the root (Mironova *et al.*, 2010; Del Bianco and Kepinski, 2011; Sassi and Vernoux, 2013). We propose that the GLV6/10 signaling pathway is an important component of this self-organizing capacity during the establishment of pre-branch sites along the primary root. When GLV6/10 peptides are in overabundance, PIN7 levels are increased throughout the xylem-pole pericycle. The increased abundance of this auxin exporter prohibits the accumulation of auxin in xylem-pole pericycle cells, including LRFCs, thereby preventing the establishment of the auxin response maxima required for LR initiation. Additionally, an excess of GLV6/10 peptides can trigger ectopic anticlinal pericycle cell divisions in an auxin independent manner. In natural conditions, however, the accumulation of auxin in LRFCs precedes and indeed triggers *GLV6/10* expression (Fernandez *et al.*, 2020; Jourquin *et al.*, 2022). In these circumstances, local auxin levels are likely sufficiently high to maintain further auxin accumulation through positive feedback mechanisms, despite the GLV-induced stimulation of auxin export. Endogenous GLV6/10 peptides are therefore unable to inhibit LR initiation in the founder cells from which they are secreted (Fig. 7). Diffusion of GLV6/10 peptides through the apoplast might create a zone around these LRFCs (or a developing primordium) where peptide levels are sufficiently high to enhance PIN7 abundance and inhibit the accumulation of auxin, thereby effectively preventing LR initiation in neighboring pericycle cells (Fig. 7). The balance between auxin and GLV6/10 peptide levels, and their spatiotemporal distributions along the pericycle, might thus create inhibitory zones around primordia in which the peptides prevent the initiation of LR primordia in close proximity to pre-existing ones. The importance of such peptide-based lateral inhibition mechanisms was recently highlighted in computational models that simulate how stable and properly spaced pre-branch sites can arise from the periodic priming of LRFCs in the elongation zone (Santos Teixeira *et al.*, 2022). In these models inhibitory peptides were assumed to suppress auxin signaling activity in neighboring XPP cells, but our data indicate that they might also reduce the actual auxin levels within these cells. In such a model, GLV6/10 peptide signaling can serve as an auxin inducible system that contributes to the robust patterning of auxin response maxima along the primary root by stimulating auxin export from XPP cells via PIN3 and PIN7.

Acknowledgements

We thank Dr. Angus Murphy for providing *abcb* mutant seeds, and Dr. Veronique Storme for advice on statistical analyses.

Author Contributions

Conceptualization, J.J., A.I.F., and T.B.; Methodology, J.J., J.S., K.L., S.V., A.I.F., and T.B.; Formal Analysis, J.J.; Investigation, J.J., K.X., Q.W., J.C., and J.S.; Resources, K.L., S.V., and T.B.; Writing-Original Draft, J.J.; Writing – Review & Editing, J.J., S.V., A.I.F., and T.B.; Visualization, J.J.; Supervision, J.J., A.I.F., S.V. and T.B.; Funding Acquisition, J.J., A.I.F., and T.B.

Conflict of Interest

No conflict of interest declared.

Funding Statement

This work was supported by doctoral (J.J., grant no. 1168218N) and postdoctoral (A.F., grant no. 1293817N) grants from the Flemish Research Foundation (FWO), an FWO project grant (A.F. grant no. G020918N, S.V. G024118N), and a China Scholarship Council grant (K.X., no. 201606350134).

Data Availability

All data supporting the findings of this study are available within the paper and the accompanying supplementary materials published online.

References

Adamowski M, Friml J. 2015. PIN-dependent auxin transport: Action, regulation, and evolution. Plant Cell **27**, 20–32.

Andersen TG, Naseer S, Ursache R, Wybouw B, Smet W, De Rybel B, Vermeer JEM, Geldner N. 2018. Diffusible repression of cytokinin signalling produces endodermal symmetry and passage cells. Nature **555**, 529–533.

Araya T, von Wirén N, Takahashi H. 2014. CLE peptides regulate lateral root development in response to nitrogen nutritional status of plants. Plant Signaling and Behavior **e29302**.

Bao Y, Aggarwal P, Robbins NE, *et al.* 2014. Plant roots use a patterning mechanism to position lateral root branches toward available water. Proceedings of the National Academy of Sciences **111**, 9319–9324.

Beeckman T, Burssens S, Inzé D. 2001. The peri-cell-cycle in Arabidopsis. Journal of experimental botany **52**, 403–411.

Beeckman T, Engler G. 1994. An easy technique for the clearing of histochemically stained plant tissue. Plant Molecular Biology Reporter **12**, 37–42.

Benková E, Michniewicz M, Sauer M, Teichmann T, Seifertová D, Jürgens G, Friml J. 2003. Local, Efflux-Dependent Auxin Gradients as a Common Module for Plant Organ Formation. Cell **115**, 591–602.

Del Bianco M, Kepinski S. 2011. Context, specificity, and self-organization in auxin response. Cold Spring Harbor Perspectives in Biology **3**, 10–20.

Billou I, Xu J, Wildwater M, Willemsen V, Paponov I, Frimi J, Heldstra R, Aida M, Palme K, Scheres B. 2005. The PIN auxin efflux facilitator network controls growth and patterning in Arabidopsis roots. Nature **433**, 39–44.

Casanova-Sáez R, Mateo-Bonmati E, Simura J, Pencik A, Novak O, Staswick P, Ljung K. 2022. Inactivation of the entire Arabidopsis group II GH3s confers tolerance to salinity and water deficit. New Phytologist **235**, 263–275.

Casimiro I, Marchant A, Bhalerao RP, *et al.* 2001. Auxin Transport Promotes Arabidopsis Lateral Root Initiation. The Plant Cell **13**, 843–852.

Chen J, Hu Y, Hao P, *et al.* 2023. ABCB-mediated shootward auxin transport feeds into the root clock. EMBO reports **e56271**.

Cho H, Ryu H, Rho S, *et al.* 2014. A secreted peptide acts on BIN2-mediated phosphorylation of ARFs to potentiate auxin response during lateral root development. Nature Cell Biology **16**, 66–76.

Czyzewicz N, Shi CL, Vu LD, van de Cotte B, Hodgman C, Butenko MA, De Smet I. 2015. Modulation of Arabidopsis and monocot root architecture by CLAVATA3/EMBRYO SURROUNDING REGION 26 peptide. Journal of Experimental Botany **66**, 5229–5243.

Dimitrov I, Tax FE. 2018. Lateral root growth in Arabidopsis is controlled by short and long distance signaling through the LRR RLKs XIP1/CEPR1 and CEPR2. Plant Signaling and Behavior **13**, 1–6.

Dong QK, Zhang ZW, Liu YT, Tao LZ, Liu HL. 2019. FERONIA regulates auxin-mediated lateral root development and primary root gravitropism. FEBS Letters **593**, 97–106.

Du Y, Scheres B. 2018. Lateral root formation and the multiple roles of auxin. Journal of Experimental Botany **69**, 155–167.

Dubrovsky JG, Doerner PW, Colón-Carmona A, Rost TL. 2000. Pericycle cell proliferation and lateral root initiation in Arabidopsis. Plant Physiology **124**, 1648–1657.

Dubrovsky JG, Sauer M, Napsucialy-Mendivil S, Ivanchenko MG, Friml J, Shishkova S, Celenza J, Benková E. 2008. Auxin acts as a local morphogenetic trigger to specify lateral root founder cells. PNAS **105**, 8790–8794.

Fernandez A, Drozdzecki A, Hoogewijs K, Nguyen A, Beeckman T, Madder A, Hilson P. 2013. Transcriptional and functional classification of the GOLVEN/ROOT GROWTH FACTOR/CLE-like signaling peptides reveals their role in lateral root and hair formation. Plant physiology **161**, 954–970.

Fernandez A, Drozdzecki A, Hoogewijs K, Vassileva V, Madder A, Beeckman T, Hilson P. 2015. The GLV6/RGF8/CLEL2 peptide regulates early pericycle divisions during lateral root initiation. Journal of Experimental Botany **66**, 5245–5256.

Fernandez AI, Vangheluwe N, Xu K, *et al.* 2020. GOLVEN peptide signalling through RGI receptors and MPK6 restricts asymmetric cell division during lateral root initiation. Nature Plants **6**, 533–543.

Ferreira PCG, Hemerly AS, de Engler JA, van Montagu M, Engler G, Inzé D. 1994. Developmental expression of the Arabidopsis cyclin gene cyc1At. Plant Cell **6**, 1763–1774.

Friml J, Wisniewska J, Benkova E, Mendgen K, Palme K. 2002. Lateral relocation of auxin efflux regulator PIN3 mediates tropism in Arabidopsis. Nature **415**, 806–809.

Fukaki H, Tameda S, Masuda H, Tasaka M. 2002. Lateral root formation is blocked by a gain-of-function mutation in the SOLITARY-ROOT/IAA14 gene of Arabidopsis. Plant Journal **29**, 153–168.

Gälweiler L, Guan C, Müller A, Wisman E, Mendgen K, Yephremov A, Palme K. 1998. Regulation of polar auxin transport by AtPIN1 in Arabidopsis vascular tissue. Science **282**, 2226–2230.

Geisler M, Aryal B, di Donato M, Hao P. 2017. A critical view on ABC transporters and their interacting partners in auxin transport. Plant and Cell Physiology **58**, 1601–1604.

Geisler M, Blakeslee JJ, Bouchard R, *et al.* 2005. Cellular efflux of auxin catalyzed by the Arabidopsis MDR/PGP transporter AtPGP1. Plant Journal **44**, 179–194.

Goh T, Joi S, Mimura T, Fukaki H. 2012*a*. The establishment of asymmetry in Arabidopsis lateral root founder cells is regulated by LBD16/ASL18 and related LBD/ASL proteins. Development **139**, 883–893.

Goh T, Kasahara H, Mimura T, Kamiya Y, Fukaki H. 2012*b*. Multiple AUX/IAA-ARF modules regulate lateral root formation: the role of Arabidopsis SHY2/IAA3-mediated auxin signalling. Philosophical Transactions of the Royal Society B: Biological Sciences **367**, 1461–1468.

Gray WM, Kepinski S, Rouse D, Leyser O, Estelle M. 2001. Auxin regulates SCFTIR1-dependent degradation of AUX/IAA proteins. Nature **414**, 271–276.

Hagen G, Guilfoyle T. 2002. Auxin-responsive gene expression: Genes, promoters and regulatory factors. Plant Molecular Biology **49**, 373–385.

Hayashi K ichiro, Arai K, Aoi Y, *et al.* 2021. The main oxidative inactivation pathway of the plant hormone auxin. Nature Communications **12**.

Himanen K, Boucheron E, Vanneste S, de Almeida Engler J, Inzé D, Beeckman T. 2002. Auxin-mediated cell cycle activation during early lateral root initiation. Plant Cell **14**, 2339–2351.

Hirota A, Kato T, Fukaki H, Aida M, Tasaka M. 2007. The Auxin-Regulated AP2/EREBP Gene PUCHI Is Required for Morphogenesis in the Early Lateral Root Primordium of Arabidopsis. The Plant Cell **19**, 2156–2168.

Hofhuis H, Laskowski M, Du Y, Prasad K, Grigg S, Pinon V, Scheres B. 2013. Phyllotaxis and rhizotaxis in Arabidopsis are modified by three plethora transcription factors. Current Biology **23**, 956–962.

Jenness MK, Carraro N, Pritchard CA, Murphy AS. 2019. The Arabidopsis ATP-BINDING CASSETTE Transporter ABCB21 Regulates Auxin Levels in Cotyledons, the Root Pericycle, and Leaves. Frontiers in Plant Science **10**, 608.

Jourquin J, Fernandez AI, Parizot B, Xu K, Grunewald W, Mamiya A, Fukaki H, Beeckman T. 2022. Two phylogenetically unrelated peptide-receptor modules jointly regulate lateral root initiation via a partially shared signaling pathway in Arabidopsis thaliana. New Phytologist **233**, 1780–1796.

Kamimoto Y, Terasaka K, Hamamoto M, *et al.* 2012. Arabidopsis ABCB21 is a facultative auxin importer/exporter regulated by cytoplasmic auxin concentration. Plant and Cell Physiology **53**, 2090–2100.

Karimi M, Bleys A, Vanderhaeghen R, Hilson P. 2007. Building blocks for plant gene assembly. Plant Physiology **145**, 1183–1191.

Karimi M, de Meyer B, Hilson P. 2005. Modular cloning in plant cells. Trends in Plant Science **10**, 103–105.

Kepinski S, Leyser O. 2005. The Arabidopsis F-box protein TIR1 is an auxin receptor. Nature **435**, 446–451.

Kleine-Vehn J, Ding Z, Jones AR, Tasaka M, Morita MT, Friml J. 2010. Gravity-induced PIN transcytosis for polarization of auxin fluxes in gravity-sensing root cells. Proceedings of the National Academy of Sciences of the United States of America **107**, 22344–22349.

Kong X, Zhang C, Zheng H, *et al.* 2020. Antagonistic Interaction between Auxin and SA Signaling Pathways Regulates Bacterial Infection through Lateral Root in Arabidopsis. Cell Reports **32**, 108060.

Kurihara D, Mizuta Y, Sato Y, Higashiyama T. 2015. ClearSee: a rapid optical clearing reagent for whole-plant fluorescence imaging. Development **142**, 4168–4179.

Laskowski M, Grieneisen VA, Hofhuis H, ten Hove CA, Hogeweg P, Marée AFM, Scheres B. 2008. Root system architecture from coupling cell shape to auxin transport. PLoS Biology **6**, 2721–2735.

Lavenus J, Goh T, Roberts I, Guyomarc'h S, Lucas M, De Smet I, Fukaki H, Beeckman T, Bennett M, Laplaze L. 2013. Lateral root development in Arabidopsis: Fifty shades of auxin. Trends in Plant Science **18**, 1360–1385.

Lenth RV. 2021. emmeans: Estimated Marginal Means, aka Least-Squares Means. R package V1.7.0. https://cran.r-project.org/package=emmeans.

Lewis DR, Negi S, Sukumar P, Muday GK. 2011. Ethylene inhibits lateral root development, increases IAA transport and expression of PIN3 and PIN7 auxin efflux carriers. Development **138**, 3485–3495.

Lin R, Wang H. 2005. Two homologous ATP-binding cassette transporter proteins, AtMDR1 and AtPGP1, regulate Arabidopsis photomorphogenesis and root development by mediating polar auxin transport. Plant Physiology **138**, 949–964.

Ljung K, Hull AK, Celenza J, Yamada M, Estelle M, Normanly J, Sandberg G. 2005. Sites and regulation of auxin biosynthesis in arabidopsis roots. Plant Cell **17**, 1090–1104.

López-Bucio J, Carlos Campos-Cuevas J, Hernández-Calderón E, Velásquez-Becerra C, Farías-Rodríguez R, Iveth Macías-Rodríguez L, Valencia-Cantero E. 2007. Bacillus megaterium Rhizobacteria Promote Growth and Alter Root-System Architecture Through an Auxin-and Ethylene-Independent Signaling Mechanism in Arabidopsis thaliana. MPMI **20**, 207–217.

López-Bucio J, Hernández-Abreu E, Sánchez-calderón L, Nieto-Jacobo FM, Simpson J, Herrera-estrella L. 2002. Phosphate Availability Alters Architecture and Causes Changes in Hormone Sensitivity in the Arabidopsis Root System. Plant Physiology **129**, 244–256.

Ludwig-Müller J. 2011. Auxin conjugates: Their role for plant development and in the evolution of land plants. Journal of Experimental Botany **62**, 1757–1773.

Malamy JE, Benfey PN. 1997. Organization and cell differentiation in lateral roots of Arabidopsis thaliana. Development **124**, 33–44.

Marchant A, Bhalerao R, Casimiro I, Eklöf J, Casero PJ, Bennett M, Sandberg G. 2002. AUX1 promotes lateral root formation by facilitating indole-3-acetic acid distribution between sink and source tissues in the Arabidopsis seedling. Plant Cell **14**, 589–597.

Marhavý P, Vanstraelen M, De Rybel B, Zhaojun D, Bennett MJ, Beeckman T, Benková E. 2013. Auxin reflux between the endodermis and pericycle promotes lateral root initiation. EMBO Journal **32**, 149–158.

Mellor N, Band LR, Pěňík A, *et al.* 2016. Dynamic regulation of auxin oxidase and conjugating enzymes AtDAO1 and GH3 modulates auxin homeostasis. Proceedings of the National Academy of Sciences of the United States of America **113**, 11022–11027.

Meng L, Buchanan BB, Feldman LJ, Luan S. 2012. CLE-like (CLEL) peptides control the pattern of root growth and lateral root development in Arabidopsis. PNAS **109**, 1760–1765.

Mi H, Muruganujan A, Huang X, Ebert D, Mills C, Guo X, Thomas PD. 2019. Protocol Update for large-scale genome and gene function analysis with the PANTHER classification system (v.14.0). Nature Protocols **14**, 703–721.

Mironova V v., Omelyanchuk NA, Yosiphon G, Fadeev SI, Kolchanov NA, Mjolsness E, Likhoshvai VA. 2010. A plausible mechanism for auxin patterning along the developing root. BMC Systems Biology **4**.

Moreno-Risueno MA, van Norman JM, Moreno A, Zhang J, Ahnert SE, Benfey PN. 2010. Oscillating gene expression determines competence for periodic Arabidopsis root branching. Science **329**, 1306–1311.

Mravec J, Kubeš M, Bielach A, Gaykova V, Petrášek J, Skupa P, Chand S, Benková E, Zažímalová E, Friml J. 2008. Interaction of PIN and PGP transport mechanisms in auxin distribution-dependent development. Development **135**, 3345–3354.

Murphy E, Vu LD, van den Broeck L, *et al.* 2016. RALFL34 regulates formative cell divisions in Arabidopsis pericycle during lateral root initiation. Journal of Experimental Botany **67**, 4863–4875.

Nakazawa M, Yabe N, Ichikawa T, Yamamoto YY, Yoshizumi T, Hasunuma K, Matsui M. 2001. DFL1, an auxin-responsive GH3 gene homologue, negatively regulates shoot cell elongation and lateral root formation, and positively regulates the light response of hypocotyl length. Plant Journal **25**, 213–221.

Noh B, Murphy AS, Spalding EP. 2001. Multidrug Resistance –like Genes of Arabidopsis Required for Auxin Transport and Auxin-Mediated Development . The Plant Cell **13**, 2441–2454.

Van Norman JM, Xuan W, Beeckman T, Benfey PN. 2013. To branch or not to branch: The role of pre-patterning in lateral root formation. Development **140**, 4301–4310.

Novák O, Hényková E, Sairanen I, Kowalczyk M, Pospíšil T, Ljung K. 2012. Tissue-specific profiling of the Arabidopsis thaliana auxin metabolome. Plant Journal **72**, 523–536.

Okushima Y, Fukaki H, Onoda M, Theologis A, Tasaka M. 2007. ARF7 and ARF19 Regulate Lateral Root Formation via Direct Activation of LBD/ASL Genes in Arabidopsis. The Plant Cell **19**, 118–130.

Okushima Y, Overvoorde PJ, Arima K, *et al.* 2005. Functional Genomic Analysis of the AUXIN RESPONSE FACTOR Gene Family Members in Arabidopsis thaliana: Unique and Overlapping Functions of ARF7 and ARF19. The Plant Cell **17**, 444–463.

Orman-Ligeza B, Morris EC, Parizot B, *et al.* 2018. The Xerobranching Response Represses Lateral Root Formation When Roots Are Not in Contact with Water. Current Biology **28**, 3165-3173.e5.

Orosa-Puente B, Leftley N, von Wangenheim D, *et al.* 2018. Root branching toward water involves posttranslational modification of transcription factor ARF7. Science **362**, 1407–1410.

Ou Y, Lu X, Zi Q, *et al.* 2016. RGF1 INSENSITIVE 1 to 5, a group of LRR receptor-like kinases, are essential for the perception of root meristem growth factor 1 in Arabidopsis thaliana. Cell Research **26**, 686–698.

Paponov IA, Paponov M, Teale W, Menges M, Chakrabortee S, Murray JAH, Palme K. 2008. Comprehensive transcriptome analysis of auxin responses in Arabidopsis. Molecular Plant **1**, 321–337.

Parizot B, Laplaze L, Ricaud L, *et al.* 2008. Diarch symmetry of the vascular bundle in arabidopsis root encompasses the pericycle and is reflected in distich lateral root initiation. Plant Physiology **146**, 140–148.

Park JE, Park JY, Kim YS, Staswick PE, Jeon J, Yun J, Kim SY, Kim J, Lee YH, Park CM. 2007. GH3-mediated auxin homeostasis links growth regulation with stress adaptation response in Arabidopsis. Journal of Biological Chemistry **282**, 10036–10046.

Parry G, Calderon-Villalobos LI, Prigge M, Peret B, Dharmasiri S, Itoh H, Lechner E, Gray WM, Bennett M, Estelle M. 2009. Complex regulation of the TIR1/AFB family of auxin receptors. Proceedings of the National Academy of Sciences of the United States of America **106**, 22540–22545.

Porco S, Pěnčík A, Rasheda A, *et al.* 2016. Dioxygenase-encoding AtDAO1 gene controls IAA oxidation and homeostasis in arabidopsis. Proceedings of the National Academy of Sciences of the United States of America **113**, 11016–11021.

R Core Team. 2020. R: A language and environment for statistical computing. R Foundation for Statistical Computing. https://www.r-project.org/ **.**

Rampey RA, LeClere S, Kowalczyk M, Ljung K, Sandberg G, Bartel B. 2004. A family of auxin-conjugate hydrolases that contributes to free indole-3-acetic acid levels during arabidopsis germination. Plant Physiology **135**, 978–988.

Roberts I, Smith S, Stes E, *et al.* 2016. CEP5 and XIP1/CEPR1 regulate lateral root initiation in Arabidopsis. Journal of Experimental Botany **67**, 4889–4899.

Roman G, Lubarsky B, Kieber JJ, Rothenberg M, Ecker JR. 1995. Genetic analysis of ethylene signal transduction in Arabidopsis thaliana: five novel mutant loci integrated into a stress response pathway. Genetics **139**, 1393–1409.

De Rosario-Martinez H. 2015. phia: Post-Hoc Interaction Analysis. R Package V0.2-1. https://cran.r-project.org/package=phia.

Ruegger M, Dewey E, Gray WM, Hobbie L, Turner J, Estelle M. 1998. The TIR1 protein of Arabidopsis functions in auxin response and is related to human SKP2 and yeast Grr1p. Genes and Development **12**, 198–207.

De Rybel B, Vassileva V, Parizot B, *et al.* 2010. A novel Aux/IAA28 signaling cascade activates GATA23-dependent specification of lateral root founder cell identity. Current Biology **20**, 1697–1706.

Santelia D, Vincenzetti V, Azzarello E, Bovet L, Fukao Y, Duchtig P, Mancuso S, Martinoia E, Geisler M. 2005. MDR-like ABC transporter AtPGP4 is involved in auxin-mediated lateral root and root hair development. FEBS Letters **579**, 5399–5406.

Santos Teixeira J, van den Berg T, ten Tusscher K. 2022. Reverse engineering lateral root stable prebranch site formation; complementary roles for auxin and auxin signalling. Development **149**, dev200927.

Sassi M, Vernoux T. 2013. Auxin and self-organization at the shoot apical meristem. Journal of Experimental Botany **64**, 2579–2592.

Savaldi-Goldstein S, Baiga TJ, Pojer F, *et al.* 2008. New auxin analogs with growth-promoting effects in intact plants reveal a chemical strategy to improve hormone delivery. Proceedings of the National Academy of Sciences of the United States of America **105**, 15190–15195.

Schindelin J, Arganda-Carreras I, Frise E, *et al.* 2012. Fiji: An open-source platform for biological-image analysis. Nature Methods **9**, 676–682.

Schneider CA, Rasband WS, Eliceiri KW. 2012. NIH Image to ImageJ: 25 years of image analysis. Nature Methods **9**, 671–675.

Shin R, Burch AY, Huppert KA, Tiwari SB, Murphy AS, Guilfoyle TJ, Schachtman DP. 2007. The Arabidopsis transcription factor MYB77 modulates auxin signal transduction. Plant Cell **19**, 2440–2453.

Šimášková M, O'Brien JA, Khan M, *et al.* 2015. Cytokinin response factors regulate PIN-FORMED auxin transporters. Nature Communications **6**, 8717.

De Smet I, Tetsumura T, De Rybel B, *et al.* 2007. Auxin-dependent regulation of lateral root positioning in the basal meristem of Arabidopsis. Development **134**, 681–690.

De Smet I, Vassileva V, De Rybel B, *et al.* 2008. Receptor-Like Kinase ACR4 Restricts Formative Cell Divisions in the Arabidopsis Root. Science **322**, 594–597.

Song W, Liu L, Wang J, *et al.* 2016. Signature motif-guided identification of receptors for peptide hormones essential for root meristem growth. Cell Research **26**, 674–685.

Staswick PE, Serban B, Rowe M, Tiryaki I, Maldonado MT, Maldonado MC, Suza W. 2005. Characterization of an Arabidopsis Enzyme Family That Conjugates Amino Acids to Indole-3-Acetic Acid. The Plant Cell **17**, 616–627.

Staswick PE, Tiryaki I, Rowe ML. 2002. Jasmonate response locus JAR1 and several related Arabidopsis genes encode enzymes of the firefly luciferase superfamily that show activity on jasmonic, salicylic, and indole-3-acetic acids in an assay for adenylation. Plant Cell **14**, 1405–1415.

Swarup K, Benková E, Swarup R, *et al.* 2008. The auxin influx carrier LAX3 promotes lateral root emergence. Nature Cell Biology **10**, 946–954.

Swarup R, Kargul J, Marchant A, *et al.* 2004. Structure-Function Analysis of the Presumptive Arabidopsis Auxin Permease AUX1. The Plant Cell **16**, 3069–3083.

Swarup R, Péret B. 2012. AUX/LAX family of auxin influx carriers-An overview. Frontiers in Plant Science **3**, 1–11.

Takase T, Nakazawa M, Ishikawa A, Kawashima M, Ichikawa T, Takahashi N, Shimada H, Manabe K, Matsui M. 2004. ydk1-D, an auxin-responsive GH3 mutant that is involved in hypocotyl and root elongation. Plant Journal **37**, 471–483.

Terasaka K, Blakeslee JJ, Titapiwatanakun B, *et al.* 2005. PGP4, an ATP binding cassette P-glycoprotein, catalyzes auxin transport in Arabidopsis thaliana roots. Plant Cell **17**, 2922–2939.

Tiwari SB, Wang XJ, Hagen G, Guilfoyle TJ. 2001. Aux/IAA proteins are active repressors, and their stability and activity are modulated by auxin. Plant Cell **13**, 2809–2822.

Toyokura K, Goh T, Shinohara H, *et al.* 2019. Lateral Inhibition by a Peptide Hormone-Receptor Cascade during Arabidopsis Lateral Root Founder Cell Formation. Developmental Cell **48**, 64–75.

Ulmasov T, Hagen G, Guilfoyle TJ. 1999. Dimerization and DNA binding of auxin response factors. Plant Journal **19**, 309–319.

Ulmasov T, Murfett J, Hagen G, Guilfoyle TJ. 1997. Aux/IAA Proteins Repress Expression of Reporter Genes Containing Natural and Highly Active Synthetic Auxin Response Elements. The Plant Cell **9**, 1963–1971.

Ursache R, Andersen TG, Marhavý P, Geldner N. 2018. A protocol for combining fluorescent proteins with histological stains for diverse cell wall components. Plant Journal **93**, 399–412.

Vanneste S, Coppens F, Lee E, *et al.* 2011. Developmental regulation of CYCA2s contributes to tissue-specific proliferation in Arabidopsis. EMBO Journal **30**, 3430–3441.

Vanneste S, De Rybel B, Beemster GTS, *et al.* 2005. Cell cycle progression in the pericycle is not sufficient for SOLITARY ROOT/IAA14-mediated lateral root initiation in Arabidopsis thaliana. Plant Cell **17**, 3035–3050.

Vernoux T, Brunoud G, Farcot E, *et al.* 2011. The auxin signalling network translates dynamic input into robust patterning at the shoot apex. Molecular Systems Biology **7**, 508.

Wang HZ, Yang KZ, Zou JJ, *et al.* 2015. Transcriptional regulation of PIN genes by FOUR LIPS and MYB88 during Arabidopsis root gravitropism. Nature Communications **6**, 8822.

Whitford R, Fernandez A, Tejos R, *et al.* 2012. GOLVEN Secretory Peptides Regulate Auxin Carrier Turnover during Plant Gravitropic Responses. Developmental Cell **22**, 678–685.

Wu G, Lewis DR, Spalding EP. 2007. Mutations in Arabidopsis Multidrug Resistance-Like ABC transporters separate the roles of acropetal and basipetal auxin transport in lateral root development. Plant Cell **19**, 1826–1837.

Xu K, Jourquin J, Xu X, De Smet I, Fernandez AI, Beeckman T. 2023. Dynamic GOLVEN-ROOT GROWTH FACTOR 1 INSENSITIVE signaling in the root cap mediates root gravitropism. Plant Physiology, kiad073.

Xuan W, Audenaert D, Parizot B, *et al.* 2015. Root cap-derived auxin pre-patterns the longitudinal axis of the arabidopsis root. Current Biology **25**, 1381–1388.

Xuan W, Band LR, Kumpf RP, *et al.* 2016. Cyclic programmed cell death stimulates hormone signaling and root development in Arabidopsis. Science **351**, 384–387.

Yang Y, Hammes UZ, Taylor CG, Schachtman DP, Nielsen E. 2006. High-Affinity Auxin Transport by the AUX1 Influx Carrier Protein. Current Biology **16**, 1123–1127.

Zamioudis C, Mastranesti P, Dhonukshe P, Blilou I, Pieterse CMJ. 2013. Unraveling root developmental programs initiated by beneficial Pseudomonas spp. Bacteria. Plant Physiology **162**, 304–318.

Zhang J, Lin JE, Harris C, Pereira FCM, Wu F, Blakeslee JJ, Peer WA. 2016. DAO1 catalyzes temporal and tissue-specific oxidative inactivation of auxin in Arabidopsis thaliana. Proceedings of the National Academy of Sciences of the United States of America **113**, 11010–11015.

Zhao Y, Christensen SK, Fankhauser C, Cashman JR, Cohen JD, Weigel D, Chory J. 2001. A Role for Flavin Monooxygenase-Like Enzymes in Auxin Biosynthesis. Science **291**, 306–309.

Figures

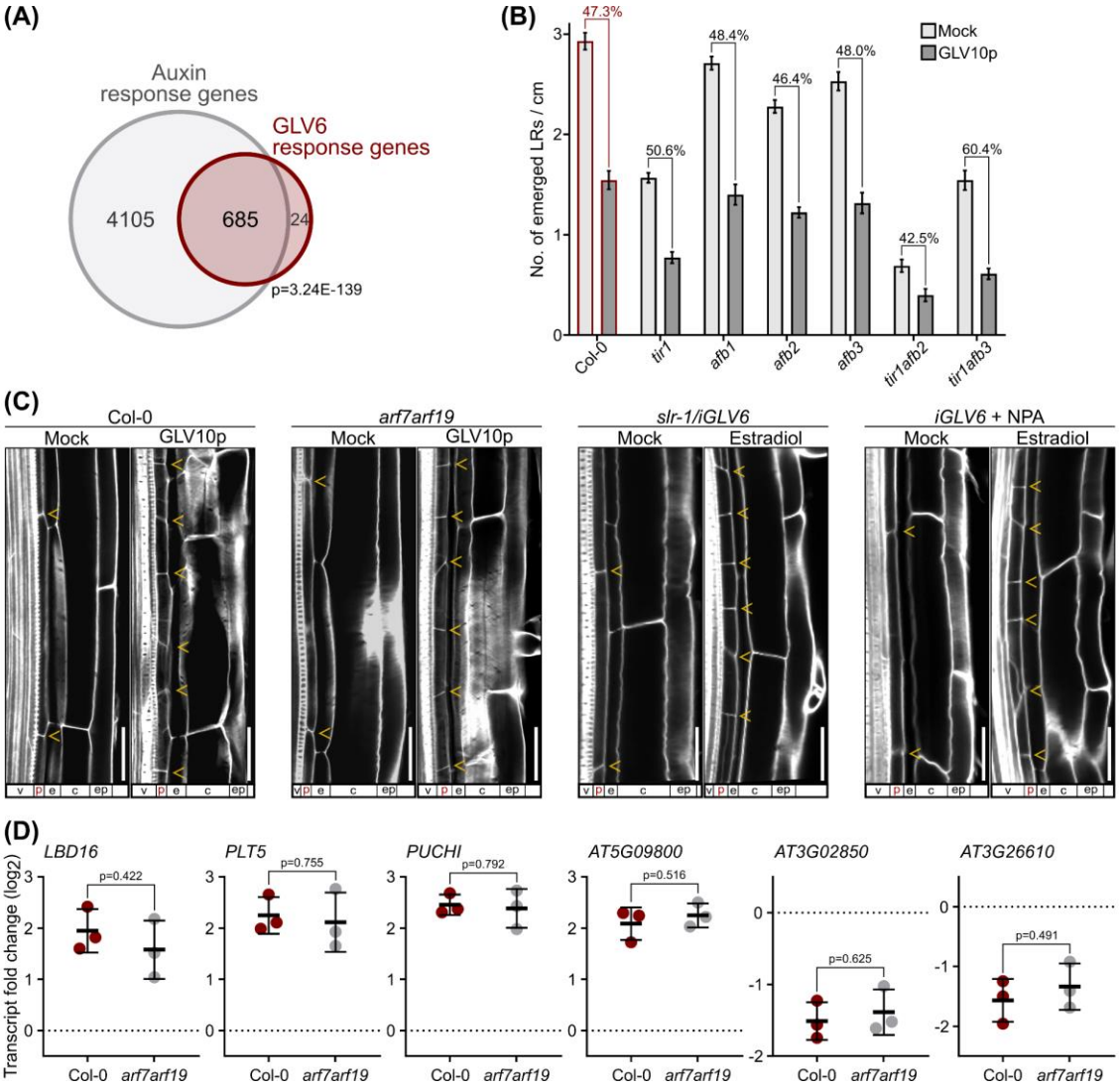

Fig. 1. GLV6/10 peptide signaling induces a partial auxin response downstream of the canonical auxin signaling pathway. **(A)** Venn diagram showing the overlap between GLV6-regulated genes and genes found to respond to NAA and/or IAA treatment in an *IAA14/SLR* and/or *ARF7ARF19* dependent manner, as shown by the microarray experiments performed by Vanneste *et al.,2005* and Okushima *et al., 2005.* A list of these genes and their transcript fold changes can be found in *supplementary table S2*. Statistical significance (p-value < 0.05) was determined via a hypergeometric test. **(B)** Emerged LR densities of 12-day old wild-type, *tir1, afb1, afb2, afb3, tir1afb2 and tir1afb3* mutant seedlings, treated or not with 100 nM GLV10p. Mean numbers of emerged LRs per centimeter primary root ± SE are shown. For each genotype, the percentual decrease in LR density as a result of GLV10p treatment is indicated. Asterisks indicate a decrease that is significantly different (p-value < 0.05) from that observed in the wild-type control (none in this case), n = 15. Statistical significance was determined via quasipoisson regression with Dunnett's correction. **(C)** Confocal images of longitudinal sections through the maturation zone of 9-day old Col-0, *arf7arf19, slr-1/iGLV6* and NPA-treated (10 µM) *iGLV6* roots, treated or not with 100 nM GLV10p or 2 µM estradiol (to induce *GLV6* overexpression) as indicated above each image. Anticlinal divisions within a single pericycle cell file are indicated with yellow arrowheads. The different tissue layers are indicated below each image; v=vasculature, p=pericycle, e=endodermis, c=cortex and ep=epidermis. Cell walls were stained with Calcofluor White. Scale bars represent 20 µm. **(D)** Log2 fold changes (FCs) in expression levels of *GLV6* response genes in wild-type and *arf7arf19* mutant roots 24h after treatment with 1 µM GLV10p. Individual datapoints and mean ± SD are shown, n = 3. Dotted lines indicate log2(FC) = 0 (i.e. no change in expression level). Statistical significance was determined using Student's t-tests.

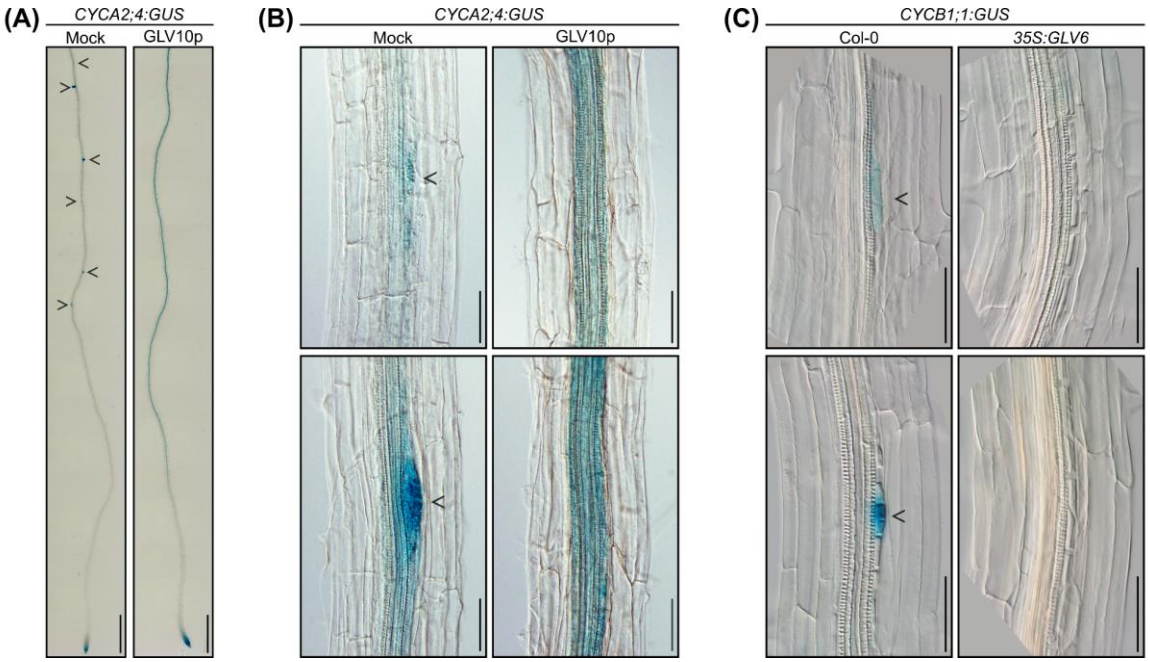

Fig. 2. GLV6/10-induced pericycle divisions differ from those induced by auxin during LR initiation. (A) *CYCA2;4:GUS* expression pattern in *Arabidopsis* roots treated or not with 200 nM GLV10p. LR primordia are highlighted with black arrowheads. Scale bars represent 0.25 cm. **(B)** Close-ups of *CYCA2;4:GUS* expression in *Arabidopsis* roots treated or not with 200 nM GLV10p. LR primordia are highlighted with black arrowheads. Scale bars represent 50 µm. **(C)** Close-ups of *CYCB1;1:GUS* expression in wild-type and *35S:GLV6 Arabidopsis* roots. LR primordia are highlighted with black arrowheads. Scale bars represent 50 µm.

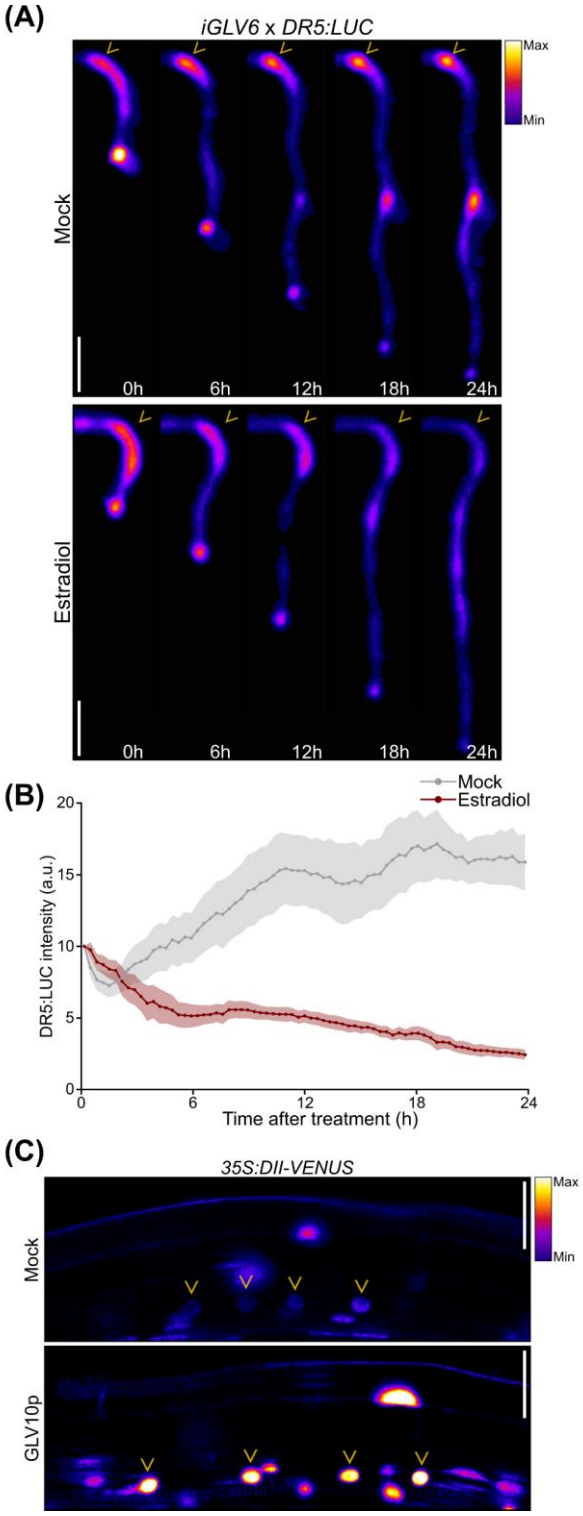

Fig. 3. GLV6/10 overabundance disrupts the accumulation of auxin in LRFCs required for LR initiation. (A) Snapshots of a 24h time course capturing LUCIFERASE activity in untreated and estradiol-treated *iGLV6/DR5:LUCIFERASE* roots. Roots were gravistimulated 8h prior to the start of the time series and *GLV6* overexpression was instigated at the onset of the time course. The locations of pre-branch sites in the root bend are marked with yellow arrowheads. LUCIFERASE intensity is shown in arbitrary units. Scale bars represent 0.2 cm. **(B)** Time course of LUCIFERASE intensity in pre-branch sites within gravistimulation-induced root bends of *iGLV6/DR5:LUC* roots treated or not with estradiol. Roots were gravistimulated 8h prior to the start of the time series and *GLV6* overexpression was instigated at the onset of the time course. LUCIFERASE intensity in each gravistimulation-induced pre-branch site was measured every 20min for 24h, and normalized against its intensity at the start of the time series, which was arbitrarily set at 10 arbitrary units (a.u.). The mean ± SE are shown, n = 10. **(C)** Representative confocal images of *35S:DII-VENUS* expression in gravistimulation-induced root bends. Roots were treated

or not with 1 µM GLV10p at 8h after gravistimulation and imaged 18h after gravistimulation. Nuclei of pericycle cells are indicated with white arrowheads. Scale bars represent 30 µm.

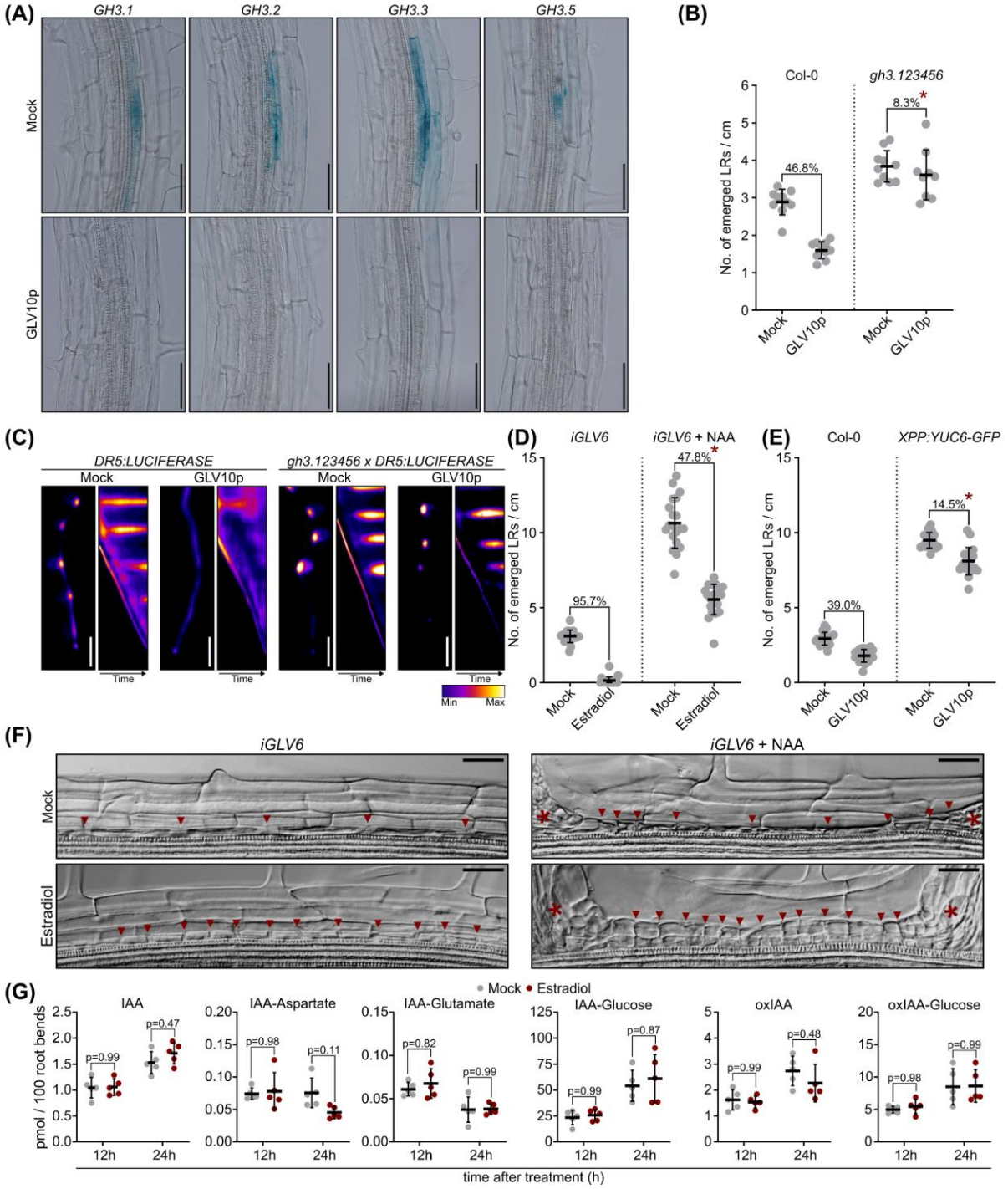

Fig. 4. Exploring the effect of GLV6/10 peptide signaling on auxin metabolism. (A) *GH3.1:GUS, GH3.2:GUS, GH3.3:GUS* and *GH3.5:GUS* expression patterns in gravistimulation-induced root bends 18h after gravistimulation and treatment with 1 µM GLV10p. Scale bars represent 50 µm. **(B)** Emerged LR densities of 12-day old wild-type and *gh3.123456* mutant seedlings, treated or not with 100 nM GLV10p. Individual datapoints and mean ± SD are shown. For each genotype, the percentual decrease in emerged LR density as a result of GLV10p treatment is indicated. Asterisks indicate a decrease that is significantly different from that observed in the wild-type control (p-value < 0.05), n = 10. Statistical significance was determined via quasipoisson regression. **(C)** Left: Snapshots of roots after an 18h time course capturing LUCIFERASE activity in *DR5:LUCIFERASE* and *gh3.123456* x *DR5:LUCIFERASE* lines, treated or not with 1 µM GLV10p at the onset of the experiment. Right: Kymopgraphs depicting LUCIFERASE intensities in each corresponding root over the 18h time course, shown in arbitrary units. Scale bars represent 0.2 cm. Additional snapshots can be found in *Supplementary Figure S7.* **(D)** Emerged LR densities of 12-day old *iGLV6* seedlings treated or not with 0.1 µM NAA and/or 2 µM estradiol to induce *GLV6* overexpression. Individual datapoints and mean ± SD are shown, n = 20. For each condition, the percentual decrease in emerged LR density as a result

of *GLV6* overexpression is indicated. Asterisks indicate a decrease that is significantly different from that observed in the NAA-free control (p-value < 0.05). Statistical significance was determined via quasipoisson regression. **(E)** Emerged LR densities of 12-day old *XPP:YUC6-GFP* seedlings, in which auxin biosynthesis is stimulated specifically in the XPP, treated or not with 100 nM GLV10p. Individual datapoints and mean ± SD are shown, n = 20. For each condition, the percentual decrease in emerged LR density as a result of GLV10p treatment is indicated. Asterisks indicate a decrease that is significantly different from that observed in the wild-type control (p-value < 0.05), n = 20. Statistical significance was determined via poisson regression. **(F)** DIC images of longitudinal sections through the maturation zone of 12-day old *iGLV6* roots treated or not with 0.1 µM NAA and/or 2 µM estradiol to induce *GLV6* overexpression. Anticlinal divisions within a single pericycle cell file are indicated with red arrowheads. LR primordia are indicated with a red asterisk. Scale bars represent 30 µm. **(G)** LC-MS/MS based profiling of the amount of IAA (indole-3-acetic acid) and its detectable derivatives in 100 root bends of gravistimulated *iGLV6* seedlings after 12h and 24h of mock (DMSO) or estradiol (2 µM) treatment to induce *GLV6* overexpression. oxIAA = 2-oxindole-3-acetic acid, n = 5. Statistical significances were assessed via a two-way ANOVA and a post-hoc Tukey test.

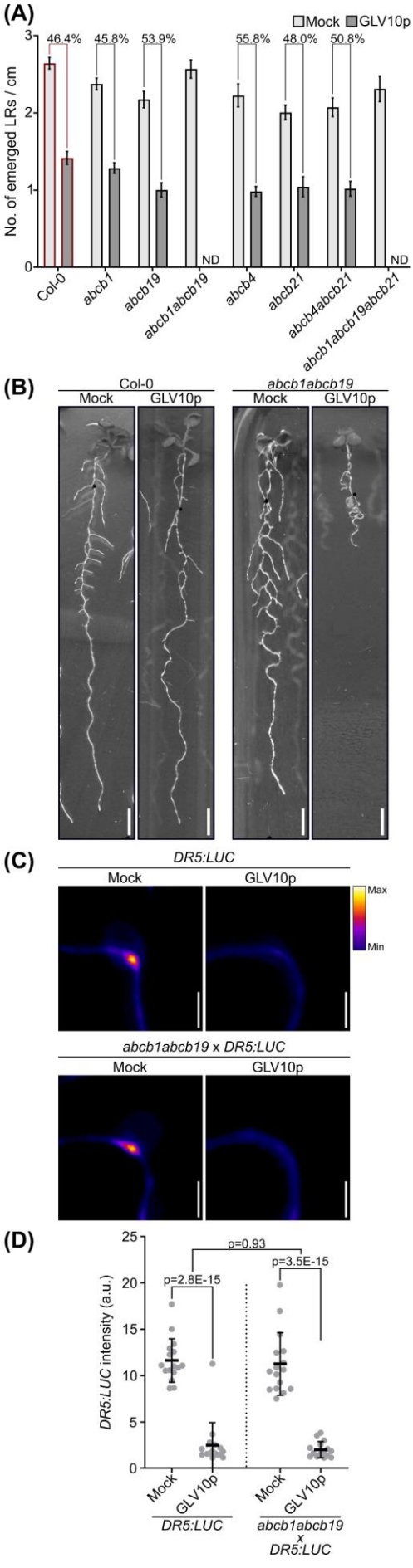
(A)
Mock
GLV10p
No. of emerged LRs / cm
46.4%
45.8%
53.9%
55.8%
48.0%
50.8%
ND
ND
Col-0
abcb1
abcb19
abcb1abcb19
abcb4
abcb21
abcb4abcb21
abcb1abcb19abcb21
(B)
Col-0
abcb1abcb19
Mock
GLV10p
(C)
DR5:LUC
Max
Min
abcb1abcb19 x DR5:LUC
(D)
DR5:LUC intensity (a.u.)
p=0.93
p=3.5E-15
p=2.8E-15
DR5:LUC
abcb1abcb19 x DR5:LUC

Fig. 5. An excess of GLV peptides perturbs primary root growth in *abcb1abcb19* mutants, but still inhibits pre-branch site formation. (A) Emerged LR densities of 12-day old wild-type and several *abcb* mutant lines, treated or not with 100 nM GLV10p. The mean numbers of emerged LRs per centimeter ± SE are shown. For each genotype, the percentual decrease in LR density as a result of GLV10p treatment is indicated. ND = not determined. Asterisks indicate a decrease that is significantly different (p-value < 0.05) from that observed in the wild-type control (none in this case), n = 15. Statistical significance was determined via quasipoisson regression with Dunnett's correction. **(B)** Representative images of the root systems of 12-day old wild-type and *abcb1abcb19* mutant seedlings, treated or not with 100 nM GLV10p. Scale bars represent 0.5 cm. **(C)** Representative images of gravistimulation-induced root bends of *DR5:LUC* and *abcb1abcb19* x *DR5:LUC* seedlings, capturing LUCIFERASE activity 24h after gravistimulation in absence or presence of 1 µM GLV10p. Luminescence intensities are shown in arbitrary units. Scale bars represent 0.2 cm. **(D)** Quantifications of *DR5:LUC* intensities in gravistimulation-induced root bends of *DR5:LUC* and *abcb1abcb19* x *DR5:LUC* seedlings, 24h after gravistimulation in absence or presence of 1 µM GLV10p. Individual datapoints and mean ± SD are shown (in arbitrary units (a.u.)). Statistical significances were determined via a two-way ANOVA and a post-hoc Tukey test, n = 16.

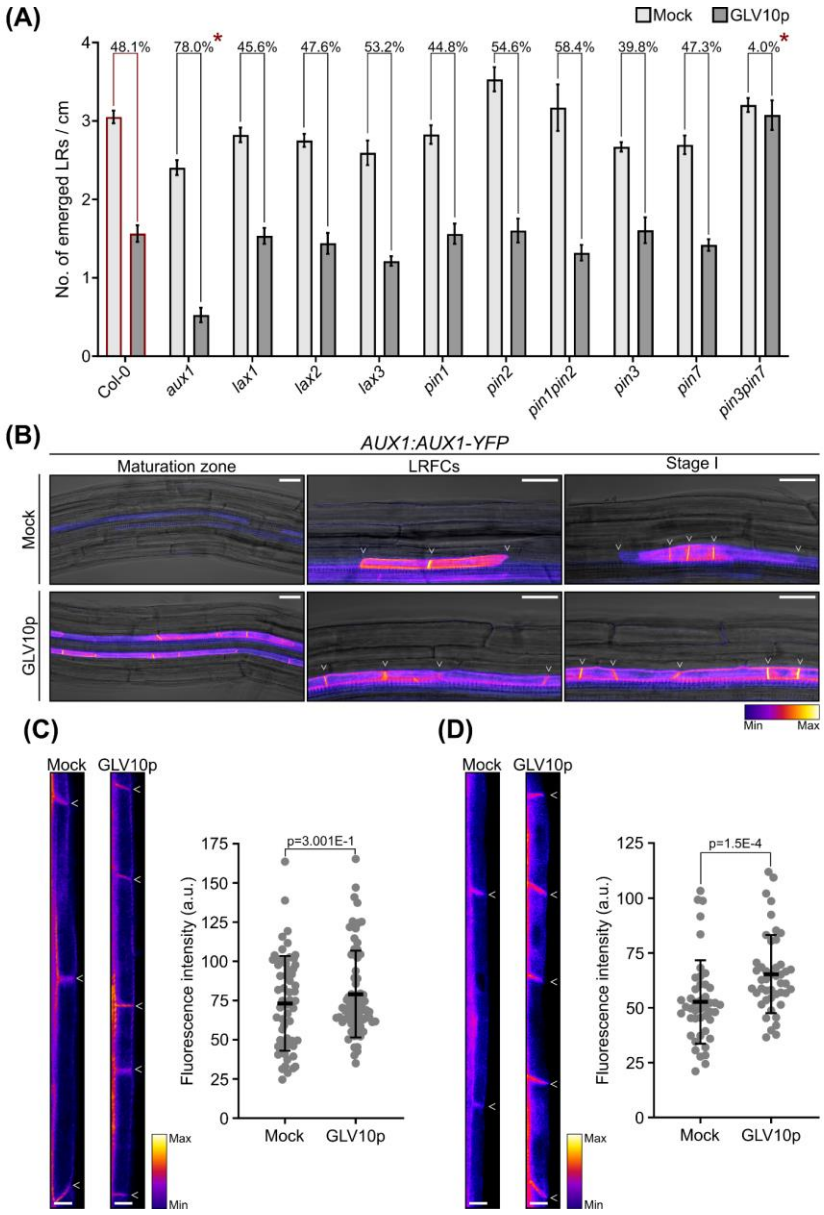

Fig. 6. Investigating the importance of (Like-)AUX1 and PIN auxin transporters for GLV6/10 signaling during LR initiation. (A) Emerged LR densities of 12-day old wild-type and several (*like-*)*aux1* and *pin* mutant lines, treated or not with 100 nM GLV10p. The mean numbers of emerged LRs per centimeter ± SE are shown. For each genotype, the percentual decrease in LR density as a result of GLV10p treatment is indicated. Asterisks indicate a decrease that is significantly different (p-value < 0.05) from that observed in the wild-type control, n = 15. Statistical significance was determined via quasipoisson regression with Dunnett's correction. **(B)** Confocal images of *AUX1:AUX1-YFP* expression in gravistimulated roots that were treated or not with 1 µM GLV10p at 8h after gravistimulation and imaged 18h after gravistimulation. Images were taken from sections

of the maturation zone above the root bends and sections within the root bends. Anticlinal cell divisions within a single pericycle cell file (undergoing LR initiation or GLV10p-induced aberrant divisions) are indicated with white arrowheads. Scale bars represent 30 µm. **(C)** Left: Confocal images of a small section of the xylem-pole pericycle in the young maturation zone of 9-day old *PIN3:PIN3-GFP* seedlings, grown in the absence or presence of 1 µM GLV10p. White arrowheads indicate anticlinal cell walls. Scale bars represent 10 µm. Right: Quantifications of the mean fluorescence intensity along anticlinal membranes of xylem-pole pericycle cells in the young maturation zone of 9-day old *PIN3:PIN3-GFP* seedlings, grown in the absence or presence of 1 µM GLV10p. Fluorescence intensities are expressed in arbitrary units (a.u.). Individual datapoints (one per anticlinal membrane) and mean ± SD are shown. Statistical significance was determined via a Mann-Whitney test. **(D)** Left: Confocal images of a small section of the xylem-pole pericycle in the young maturation zone of 9-day old *PIN7:PIN7-GFP* seedlings, grown in the absence or presence of 1 µM GLV10p. White arrowheads indicate anticlinal cell walls. Scale bars represent 10 µm. Right: Quantifications of the mean fluorescence intensity along anticlinal membranes of xylem-pole pericycle cells in the young maturation zone of 9-day old *PIN7:PIN7-GFP* seedlings, grown in the absence or presence of 1 µM GLV10p. Fluorescence intensities are expressed in arbitrary units (a.u.). Individual datapoints (one per anticlinal membrane) and mean ± SD are shown. Statistical significance was determined via a Mann-Whitney test.

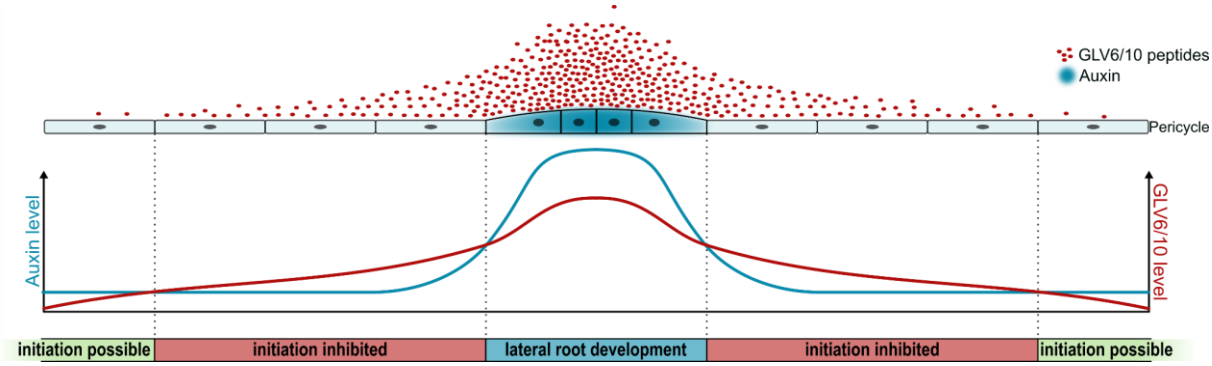

Fig. 7. Proposed model of the role of GLV6/10 signaling during LR initiation in relation to auxin. Model for the regulation of LR initiation and spacing via the balance between auxin and GLV6/10 peptide levels. The accumulation of auxin in LRFCs induces the expression of *GLV6* and *GLV10*, resulting in the secretion of GLV6/10 peptides into the apoplast. Here they diffuse outward, creating a concentration gradient around the initial pair of LRFCs. Within these LRFCs, the high auxin/GLV ratio permits further accumulation of auxin, and the effect of GLV6/10 peptides on pericycle cell divisions might even aid in the correct patterning and/or the progress of the initial LRFC divisions. Around the initiation site, a zone is created in which the low auxin/GLV ratio inhibits the accumulation of auxin in pericycle cells, most probably via the GLV-induced increase in PIN7 abundance. As a result, the initiation of new LR primordia within this zone is inhibited. Further outward, this inhibitory zone is flanked by zones in which GLV6/10 levels are sufficiently low to allow for LR initiation.